**Atmospheric
Chemistry
and Physics
Discussions**

**Part 2: Sources of
reactive bromine –
Bromocarbons**

A. Kerkweg et al.

Consistent simulation of bromine chemistry from the marine boundary layer to the stratosphere – Part 2: Bromocarbons

A. Kerkweg[1,2], P. Jöckel[1], N. Warwick[3], S. Gebhardt[1], C.A.M. Brenninkmeijer[1], and J. Lelieveld[1]

[1]Atmospheric Chemistry Department, Max Planck Institute of Chemistry, P.O. Box 3060, 55020 Mainz, Germany
[2]Institute for Atmospheric Physics, University of Mainz, Germany
[3]University of Cambridge, Chemistry Department, Lensfield Road, Cambridge, CB2 1EW, UK

Title Page	
Abstract	Introduction
Conclusions	References
Tables	Figures
◀◀	▶▶
◀	▶
Back	Close
Full Screen / Esc	
Printer-friendly Version	
Interactive Discussion	

Abstract

In this second part of a series of articles dedicated to a detailed analysis of bromine chemistry in the atmosphere we address one (out of two) dominant natural sources of reactive bromine. The two main source categories are the release of bromine from sea salt and the decomposition of bromocarbons by photolysis and reaction with OH. Here, we focus on C_1-bromocarbons. We show that the atmospheric chemistry general circulation model ECHAM5/MESSy realistically simulates their emission, transport and decomposition from the boundary layer up to the mesosphere. We included oceanic emission fluxes of the short-lived bromocarbons CH_2Br_2, CH_2ClBr, $CHClBr_2$, $CHCl_2Br$, $CHBr_3$ and of CH_3Br. The vertical profiles and the surface mixing ratios of the bromocarbons are in general agreement with the (few available) observations, especially in view of the limited information available and the consequent coarseness of the emission fields. For $CHBr_3$, $CHCl_2Br$ and $CHClBr_2$ photolysis is the most important degradation process in the troposphere. In contrast to this, tropospheric CH_2Br_2, CH_3Br and CH_2ClBr are more efficiently decomposed by reaction with OH. In the free troposphere approximately one third of the C_1-bromocarbons decomposes by reaction with OH. In the boundary layer the reaction with OH is relatively important, whereas it is negligible in the stratosphere. Our results indicate an approximately 50% longer lifetime of CH_3Br ($\approx$1 year) than assumed previously, implying a relatively strong contribution to stratospheric bromine and consequent ozone destruction.

1 Introduction

The abundance of bromine in the troposphere and the importance of individual bromine sources to atmospheric halogen chemistry is highly uncertain. Only few measurement data of reactive bromine precursors are available. The main sources are the release of inorganic bromine from sea salt and emissions of bromocarbons followed by photolysis or reaction with OH. In the present study about atmospheric bromine, the focus is

on C_1-bromocarbons (further denotes as bromocarbons). Their emission fluxes, the transport and the main regions and processes of degradation are investigated here.

The most comprehensive model studies of bromocarbons thus far have been performed by Warwick et al. (2006a,b) who applied the Chemical Transport Model (CTM)
p-TOMCAT to simulate atmospheric bromoform ($CHBr_3$) and other short-lived bromocarbons. (Table 1 lists all abbreviations.) They concluded that global source estimates using the previously used top-down approach were too low and suggested a global emission flux of about 400-600 Gg($CHBr_3$)/yr. These emissions largely take place in the tropics. In addition to bromoform, Warwick et al. (2006a) investigated the short-
lived bromocarbons CH_2Br_2, CH_2ClBr, $CHClBr_2$, and $CHCl_2Br$. The emission fields of these compounds have been scaled to the emission fields of bromoform. Yang et al. (2005) were the first to use these emission fields to simulate bromine chemistry in the troposphere together with semi-prognostically calculated bromine sources from sea-salt aerosol, also using the p-TOMCAT model.

In this study we apply the emission fields proposed by Warwick et al. (2006a) in our atmospheric chemistry general circulation model (AC-GCM). As the GCM is only weakly forced towards the analysed meteorology of the European Centre for Medium-Range Weather Forecasts (ECMWF), it consistently calculates its own meteorology, whereas p-TOMCAT is driven offline by 6-hourly ECMWF data. Furthermore, our model
also includes the middle atmosphere and realistically simulates the exchange between stratosphere and troposphere (STE) in the applied vertical resolution. The p-TOMCAT model domain, in contrast, is restricted to below 30 km altitude. Hence, some differences between the simulated bromocarbon distributions in our simulation and those of Warwick et al. (2006a) and Yang et al. (2005) are to be expected.

Only few measurement data sets are available for an evaluation of the simulation results. Surface mixing ratios have often been observed in coastal regions, but in these locations bromocarbon emissions are usually higher than over the open ocean. Thus, many measurements have to be interpreted as upper limits, as coastlines and surf effects can not be resolved in a model with a horizontal resolution of approximately

250 km. Information about the vertical distribution of bromocarbons is even harder to obtain, since satellite observations of these species are not available. Thus the only source of height information are aircraft measurements. The three data sets used here are from CARIBIC (Brenninkmeijer et al., 1999), the Pacific Exploratory Mission (PEM): PEM-West B (Hoell et al., 1997), PEM-Tropics A (Hoell et al., 1999) and PEM-Tropics B (Raper et al., 2001) and the GABRIEL (Stickler et al., 2007; Lelieveld et al., 2008) campaign.

Section 2 describes the model setup. In Sect. 3 the simulated distributions of $CHBr_3$, CH_2Br_2, CH_2ClBr, $CHClBr_2$, $CHCl_2Br$ and CH_3Br are evaluated. The relative importance of photolysis and the reaction with OH of the bromocarbons as a source of reactive bromine is discussed in Sect. 4. Finally, the results are summarised in Sect. 5.

2 Model description

For the first comprehensive study of bromine chemistry in the boundary layer (BL), the free troposphere (FT) and the stratosphere, the ECHAM5/MESSy1$^+$ (E5/M1$^+$) model is applied. The model system consists of the general circulation model ECHAM5 (Roeckner et al., 2003, 2004, 2006) and the Modular Earth Submodel System (MESSy, Jöckel et al., 2005, 2006). For this study the middle atmosphere setup of ECHAM5, (MAECHAM5 Giorgetta et al., 2002, 2006) has been applied in the T42L87 resolution, i.e., with a triangular truncation at wave number 42 for the spectral core of ECHAM5. This corresponds to a quadratic Gaussian grid of approximately 2.8° × 2.8° in latitude and longitude, with 87 vertical levels on a hybrid-pressure grid, reaching up to 0.01 hPa (middle of the uppermost layer). The model time step is 720 s. Instantaneous data output is triggered every five hours.

The following submodels included in MESSy were switched on: cloud formation (submodel CLOUD), convection (CONVECT; Tost et al., 2006b, 2007b), convective tracer transport (CVTRANS), scavenging of trace gases and aerosols and wet deposition (SCAV; Tost et al., 2006a), gas and aerosol phase chemistry (MECCA(-AERO);

Sander et al., 2005; Kerkweg et al., 2007), photolysis (JVAL; Landgraf and Crutzen, 1998) and heterogeneous chemistry in the stratosphere (HETCHEM), online and of-fline emissions as well as tracer nudging (ONLEM, OFFLEM and TNUDGE; Kerkweg et al., 2006b), the air-sea exchange of acetone and methanol (AIRSEA; Pozzer et al., 2006), emission of NO_x from lightning (LNOX; Tost et al., 2007a), aerosol dynamics (M7; Vignati et al., 2004; Kerkweg et al., 2008), dry deposition of trace gases and aerosols (DRYDEP; Kerkweg et al., 2006a) calculated following the big leaf approach of Wesely (1989), sedimentation of aerosols (SEDI; Kerkweg et al., 2006a), radiation feedback (RAD4ALL), nudging of the QBO (QBO), polar stratospheric clouds (PSC) and TROPOP (used to determine the tropopause and the boundary layer height).

The individual submodels of the setup are described by Jöckel et al. (2006) and Kerkweg et al. (2008). Previously, atmospheric bromine was represented by prescribing CH_3Br and halon mixing ratios (CH_3Cl, $CFCl_3$, CH_3CCl_3, CCl_4, CF_2BrCl, CF_3Br) at the surface based on observations (Jöckel et al., 2006), whereas in the present study five additional bromocarbons are taken into account. In the following details are given for the submodels which are of special importance for the current study.

Bromocarbon emissions are included using the annually averaged emission fields as provided by Warwick et al. (2006a). They are processed by the submodel OFFLEM (Kerkweg et al., 2006b). Figure 1 shows the emission fields for CH_2ClBr and bromoform ($CHBr_3$). The emission fluxes of $CHCl_2Br$, CH_2Br_2 and $CHClBr_2$ show the same global pattern as CH_2ClBr. They are scaled by a constant factor yielding the annual global emission fluxes as proposed by Warwick et al. (2006a). These values are listed in Table 2. It is assumed that the bromocarbon emissions are highest in the tropics, decrease towards the mid-latitudes and approach zero at high-latitudes (>50° N or S). For bromoform, additionally enhanced coastal emissions are assumed which result in a slightly different emission pattern for $CHBr_3$. For methyl bromide pseudo-emissions are calculate using the submodel TNUDGE which is designed to nudge trace gases whose emissions are not well known but whose surface concentrations are observed. The technique of tracer nudging is described in Kerkweg et al. (2006b). In case of CH_3Br

the observations from the measurement stations of the AGAGE database (Prinn et al., 2000) are expanded into the respective surrounding latitudinal band yielding monthly latitudinal averages. Figure 2 shows the surface CH_3Br mixing ratios which are used as input for the TNUDGE submodel.

5   To evaluate the relative importance of photolysis and reaction with OH for bromocarbon degradation, diagnostic tracers are introduced to track the yields of Br radicals by photolysis of the six bromocarbons and by their reactions with OH. The supplement of this article comprises a full list of all reactions taken into account in the chemistry mechanism of MECCA (Sander et al., 2005; Kerkweg et al., 2007). The rate coeffi-
10   cients for the reactions of the bromocarbons with OH (equations G7404 to G7408 in the supplement) have been estimated by Yang et al. (2005). Their photolysis rates have been included following the suggestions of Sander et al. (2003).

The simulation period is 3 years (January 1998 to December 2000). The first two years are taken as model spin up, whereas the year 2000 is analysed. As chemistry
15   calculations which include gas and aerosol phase reactions are computationally very expensive, simulations of longer periods are not yet feasible. One simulation month took approximately 14 h wall clock time on 256 CPUs of the IBM pSeries Regatta system, based on Power 4 processor technology at the Rechenzentrum Garching (RZG).

3   Comparison of bromocarbon distributions

20   Bromocarbon observations are scarce because these compounds are difficult to measure and the interest to study them has been limited. We concentrate on the comparison with observations in the midlatitudes and tropics, as a meaningful comparison with high-latitude (polar) data would require a model which is much more adjusted to the specific needs of polar chemistry simulation. Most observations are limited to CH_3Br
25   and $CHBr_3$. We start with the investigation of the species with the shortest lifetime, $CHBr_3$, followed by the analysis of the distributions of CH_2Br_2, CH_2ClBr, $CHCl_2Br$ and $CHClBr_2$. We complete this section with the analysis of methyl bromide, the compound

with the longest lifetime of the six investigated bromocarbons.

3.1 CHBr$_3$

Bromoform is the shortest-lived bromocarbon addressed here with a lifetime of approximately 3 weeks. Figure 3 presents the simulated annual average surface mixing ratios of bromoform in pmol/mol for the year 2000. Measurements of surface CHBr$_3$ are reported more often than for other short-lived bromocarbons. Surface CHBr$_3$ was measured by Yokouchi et al. (1997) during two western Pacific cruises (one from 31 January 1991, to 20 February 1991, in the area of approximately 135–165° E, 25° S to 40° N; and one from 16 September to 25 October 1992, in the area of 135–180° E, 40° S to 40° N). They report mixing ratios between 0.13 and 2.9 pmol/mol for the western Pacific cruises. For this region, the CHBr$_3$ mixing ratios in the simulation are higher reaching values between 0.14 and 33 pmol/mol with an average of 1.9 pmol/mol. The same holds for the Asian cruise with maxima of 7.1 pmol/mol and 10 pmol/mol for the observations and the simulation, respectively. Carpenter et al. (1999) observed bromoform at Mace Head, Ireland (53° 19′ N, 9° 54′ W) during May, 1997. The bromoform mixing ratios ranged from 1.9 to 16.3 pmol/mol with an average of 6.3 pmol/mol. Two factors contribute to these relatively high mixing ratios. First, the biological seasonal cycle induces higher bromoform mixing ratios (Carpenter et al., 2005) during summer (from mid-March to mid-October: on average 5.3 pmol/mol) and lower ones in winter (mid-October to mid-March: on average 1.8 pmol/mol). Thus, the mixing ratio measured by Carpenter et al. (1999) is at the high end of what is to be expected in summer at Mace Head. Second, Mace Head is a well-known coastal source region for bromocarbons. Carpenter and Liss (2000) observed bromoform at Mace Head during the PARFORCE campaign (average: 6.8 pmol/mol; 1.0–22.7 pmol/mol) and at Cape Grim, Tasmania during SOAPEX 2 (average: 2.6 pmol/mol; 0.6–8.0 pmol/mol) (Carpenter et al., 2003). Our simulated surface mixing ratios for this region are near the low end of this range possibly because of the coarse model resolution as there is no distinction between coastal zones and the open sea. Ramacher et al. (1999)

observed bromoform in Ny Ålesund, Norway (78°55′ N 11°56′ E) and report an average of 0.65 pmol/mol. The measurements range from below the detection limit up to 1.0 pmol/mol. Our simulation agrees well with these measurements.

The only available data for a comparison of the vertical profiles are those from the PEM-Tropics A and B campaigns (Emmons et al., 2000; Colman et al., 2001; Blake et al., 2001). Figure 4 shows the simulated vertical profiles for bromoform (black line) compared to the PEM-Tropics A data (red dots). The profiles for the PEM-Tropics B campaign are very similar and not shown here. Since this simulation was performed for the year 2000 only, we show values for this year. The solid line indicates a spatiotemporal average for the respective flight. The dashed lines indicate the simulated minimum and maximum values during the campaign. Near the surface the simulation matches the shape of the observations, i.e. an increase towards the surface with decreasing altitude in most profiles. In contrast, the upper parts of the profiles do not match well. In the observations the mixing ratios mostly decrease towards higher altitudes, whereas most simulated profiles increase towards the tropopause. This is also in contradiction to measurements of the NASA START campaign (Schauffler et al., 1998). During this campaign in January/February, July/August and December 1996 most bromocarbons discussed here were measured in the tropical tropopause region. Schauffler et al. (1998) found bromoform to cluster at or below 0.2 pmol/mol in the upper tropical troposphere. Our simulation reaches values as high as 2 pmol/mol. The overestimation of the vertical profiles in the upper troposphere and at the tropical tropopause layer is most probably due to dynamical reasons and the emission assumption, as we can exclude chemistry, e.g. too slow reaction with OH or photolysis, as reason for the partly overestimated mixing ratios in the upper troposphere, because the simulated lifetime of $CHBr_3$ (Table 2) is by 6 days shorter as the lifetime of 26 days reported by the WMO (WMO, 2007). There are two reasons adding up yielding this too high bromoform mixing ratios. First, the emission flux of $CHBr_3$ is too high, as almost all simulated profiles show a consistently higher bromoform mixing ratio as the observations. This is most probably due to our decision to use the largest emission flux scenario proposed by War-

Part 2: Sources of reactive bromine – Bromocarbons

A. Kerkweg et al.

wick et al. (2006b), which seems to overestimate the emissions in case of our model. Second, a detailed analysis of the vertical velocity fields at all the dates and places of the vertical profiles of PEM-Tropics A showed that all c-shaped profiles are associated with large scale downward motion which is mostly attributed to the Hadley cell circu-
lation. Obviously, this motion transports bromoform downward into the upper to free troposphere. As the only source of bromoform is emission at the surface, it must have been transported upward by convection, i.e. in the upward branch of the Hadley cell circulation. Thus convection plays an important role for the simulated overestimation in the upper troposphere. But the convection scheme by Tiedtke does not overestimate
neither convection intensity or height nor the frequence at which convection is triggered (Tost et al., 2006b). Hence, due to the high bromoform emission simply to much bromoform is transported upward by convection and leads to too high bromoform mixing ratios in the subsidence area of the Hadley cell. This is confirmed by the fact, that all regions which recently have been subject to convection show an overestimation of the
bromoform mixing ratios in the lower and middle troposphere. These regions can be identified by their well mixed profiles.

3.2 CH_2Br_2

The number of measurements for dibromomethane is very limited. Yokouchi et al. (1997) measured surface CH_2Br_2 during their western Pacific cruises in the range of
0.14 pmol/mol to 1.58 pmol/mol. Figure 5 displays the simulated annually averaged surface mixing ratios of CH_2Br_2. They are well within the range of the measurements of Yokouchi et al. (1997).
   Ramacher et al. (1999) observed 0.9–1.3 pmol/mol near Ny Ålesund, Norway during 29 March to 15 May 1996. At this location the simulation shows an average of
0.9 pmol/mol over the period from 29 March to 15 May 2000. This is at the lower end of the observed range. Ny Ålesund is located directly at the coast where CH_2Br_2 emissions are usually higher. Thus a single point measurement taken directly at the coast is likely to give higher mixing ratios than the average for a model grid-box of

Part 2: Sources of reactive bromine – Bromocarbons

A. Kerkweg et al.

≈250 km length. The same holds for the observations of Carpenter et al. (2003). They report CH_2Br_2 mixing ratios ranging from 0.28 to 3.39 pmol/mol with an average of 1.44 pmol/mol at Mace Head during the PARFORCE campaign (September 1998). This is again about a factor of 2 more CH_2Br_2 than predicted by the simulation.

5   In contrast, the simulated southern hemispheric mixing ratios are slightly too high. During the SOAPEX 2 campaign Carpenter et al. (2003) observed average CH_2Br_2 mixing ratios of 0.43 pmol/mol, varying between 0.1 and 1.39 pmol/mol. For January/February 2000, the simulation shows an average mixing ratio of 1.2 pmol/mol, which is well within the range of measured values but significantly higher than the ob-
10 served mean value.

To evaluate the vertical distribution of CH_2Br_2 aircraft measurements are required. The aircraft measurement campaigns PEM-Tropics-A and B (Colman et al., 2001) and the project CARIBIC provide the only available databases for CH_2Br_2 measurements. Colman et al. (2001) observed CH_2Br_2 mixing ratios between 0.41 and 2.55 pmol/mol
15 for the PEM-Tropics A campaign. Figure 6 shows the vertical profiles of CH_2Br_2 mixing ratios for the PEM-Tropics B campaign. The simulation overestimates CH_2Br_2 in all profiles. The observations are mostly below the interval determined by the minimum and maximum values in the model for the whole period of the measurement campaign. Nevertheless, the mixing ratios usually increase towards the surface in the simulation
20 and in the measurements. The comparison of the vertical profiles to the PEM-Tropics A data is similar and therefore not shown here.

The second collection of CH_2Br_2 aircraft measurements used is from the CARIBIC database (Oram et al., in preparation[1], Brenninkmeijer et al. (1999)). Figure 7 shows the comparison of the simulation (black line) with the CARIBIC data (red line) for eight
25 flights in 2000. The simulation overestimates the amount of CH_2Br_2 at cruising altitude (≈9–11 km) by a factor of approximately 1.5. As a consequence of the rather coarse

---

[1]Oram, D. E., Sturrock, G. A., Penkett, S. A., and Brenninkmeijer, C. A. M.: Distribution of halocarbons in the UTLS: overview of results from the CARIBIC experiment, 1997–2002, in preparation, 2008.

horizontal resolution of the model setup, the variability in time is smaller in all simulations compared to the observations, partly also because averaging over the model grid-boxes smoothes small scale variations.

In addition to these aircraft observations for which the data can be used for a direct comparison, some measurement data are available in the literature. Schauffler et al. (1993) measured a range of 0.15 to 1.02 pmol/mol, with an average of 0.72 pmol/mol during the AASE-II campaign at a flight altitude between 15.3 and 17.2 km. For the same area, the model predicts CH_2Br_2 mixing ratios of about 0.55 pmol/mol with a range from 0.11 to 0.9 pmol/mol. This matches the measurements by Schauffler et al. (1993), even though the average may be too low. Kourtidis et al. (1996) published three vertical profiles of CH_2Br_2. One was measured over Hyderabad, India (17.5° N) on 9 April 1990, the others were measured over Kiruna, Sweden (68° N). Figure 8 displays these measurements and the profiles resulting from the simulation on the same date, though for the year 2000. The thin black lines indicate the minimum and the maximum mixing ratios of the simulation in a 14-day interval centered at the respective observation dates. This provides a rough estimate of the variability at this time of year. However, the variability of the model is not high enough to explain the measurements. For Hyderabad (left), the shape of the model profile matches the observations relatively well, but the absolute values are too high. Apart from the low value at 10 km altitude, the gradient at the tropopause is relatively well captured. For January over Kiruna (middle) the simulated mixing ratios are lower by less than a factor of 2 for the measurements above the detection limit. In contrast, the simulation is off by a factor of 2 for March, 7. The steep gradient in the measurements is also found in the simulation, though at a higher altitude. This might be due to the offset of the tropopause height of the model ($\approx$9 km) compared to the observed tropopause height of 7.2 km.

Figure 9 shows the seasonal cycle of the vertical distribution of CH_2Br_2. The CH_2Br_2 concentrations are highest in the southern hemisphere. The mixing ratio decrease in the northern summer hemisphere is much more pronounced than in the southern hemisphere. This is due to the distribution of the sources and sinks of CH_2Br_2. First,

the emission fluxes of CH_2Br_2 are assumed to be only oceanic and symmetric around the Equator. Since a larger part of the southern hemisphere is covered by the ocean, the total emissions are larger. Second, the losses by photolysis and reaction with OH give rise to a seasonal cycle. The zonally averaged vertical distributions of OH concentrations in $10^6/cm^3$ are given in Fig. 10. The concentration of OH is higher in the northern hemispheric summer than in the southern hemispheric summer, thus the oxidation of CH_2Br_2 by OH is stronger in the northern hemisphere. Schauffler et al. (1998) measured on average 0.5 (±0.2) pmol/mol in the tropical tropopause region. Figure 9 suggests that the model overestimates this mixing ratio by a factor of 2, depending on the position of the tropopause (the black line in the picture indicates the average position for this time interval).

3.3 $CHClBr_2$, $CHCl_2Br$ and CH_2ClBr

Knowledge about these short-lived bromocarbons is sparse. Therefore, their emissions were scaled to the oceanic bromoform emissions according to the estimated global annual emission flux (see Table 2) as proposed by Warwick et al. (2006a).

Surface measurements are available only for $CHClBr_2$. Carpenter et al. (1999) report mixing ratios between 0.3 and 1.8 pmol/mol with an average of 0.8 pmol/mol for Mace Head, Ireland, whereas Schall and Heumann (1993) observed between < 0.01 and 1.0 pmol/mol in Spitsbergen, Norway, with an average of 0.33 pmol/mol. The left panel of Fig. 11 presents the simulated annual average surface mixing ratios of $CHClBr_2$. The simulation agrees to the observations fairly well. No surface measurements are – to our knowledge – available for $CHCl_2Br$ and CH_2ClBr. However, to give a full picture the simulated surface mixing ratios (in pmol/mol) are shown in the middle and right panels of Fig. 11, respectively.

Figure 12 shows the seasonal cycle of the vertical distributions (in fmol/mol) of $CHClBr_2$ (top), $CHCl_2Br$ (middle) and CH_2ClBr (bottom). The southern hemispheric mixing ratios of all three bromocarbons are higher than the northern hemispheric ones except for DJF. The gradient is largest during the northern hemispheric summer. Gen-

erally, due to the higher irradiation the photolysis rates and the OH concentration are higher in summer leading to a higher rate of decomposition of the bromocarbons. During the STRAT campaign Schauffler et al. (1998) measured $CHClBr_2$, $CHCl_2Br$ and CH_2ClBr mixing ratios in the tropical tropopause of about 40, 20 and 120 fmol/mol, respectively. These values are for $CHClBr_2$ and CH_2ClBr in general agreement with the average mixing ratios as shown in Fig. 12 whereas the $CHCl_2Br$ mixing ratio in the tropical tropopause is up to a factor of 3 larger than measured by Schauffler et al. (1998).

The only available vertical profiles from aircraft measurements for these three compounds are from the PEM-Tropics A and B campaign (Emmons et al., 2000; Colman et al., 2001; Blake et al., 2001). Figure 13 presents the vertical profiles for $CHClBr_2$ measured during the PEM-Tropics B campaign. The observations and the simulation agree well. The picture for the PEM-Tropics A campaign is very similar and thus not shown here. Figures 14 and 15 show a comparison of the observed and simulated $CHCl_2Br$ vertical profiles during PEM-Tropics A and PEM-Tropics B, respectively. For PEM-Tropics B the model underestimates the $CHCl_2Br$ mixing ratios, whereas for PEM-Tropics A they are slightly overestimated. The model tends to simulate increasing mixing ratios towards the surface, which is not always evident in the observations. CH_2ClBr measurements are only available for PEM-Tropics B. Figure 16 shows the vertical profiles. The simulation underestimates the CH_2ClBr mixing ratio by up to a factor of 2. At the beginning and the end of the PEM-Tropics B campaign the observed mixing ratios of CH_2ClBr and $CHCl_2Br$ are very high. The feature is not covered by the simulation indicating a sofar unknown source process of CH_2ClBr and $CHCl_2Br$.

In general, no systematic model biases are apparent from Fig. 13 – 16 and the observations seem well captured. Some of the model-measurement discrepancies may be attributed to the simplified emission distribution of $CHClBr_2$, $CHCl_2Br$ and CH_2ClBr rather than to their overall emission strength.

3.4 CH$_3$Br

Methyl bromide is the longest-lived species of all six bromocarbons investigated here, and relatively many measurement data are available. Andreae et al. (1996) measured 10 to 60 pmol/mol of methyl bromide in air influenced by forest fires. This may be con-
5   sidered as an upper limit as methyl bromide is enhanced in biomass burning plumes. At Mace Head Carpenter et al. (1999) observed a mean methyl bromide mixing ratio of 13.9 pmol/mol, with a range from 9.3 to 26.1 pmol/mol. Since the coastal region near Mace Head is known to be a strong source of bromocarbons, these mixing ratios probably also represent upper limits for methyl bromide from the viewpoint of the model
10 grid scale of about 250 km. Similar values – also measured in coastal regions –, i.e. a mean of 13.7 pmol/mol (10.6–17 pmol/mol), are reported by Ramacher et al. (1999) for Ny Ålesund. Gros et al. (2003) measured 12 (±3) pmol/mol in Finokalia (35° 19° N 25°40° E) during the MINOS campaign. Simmonds et al. (2004) observed mixing ratios of 10.37 (±0.05) pmol/mol methyl bromide at Mace Head and considerably lower
15 mixing ratios with a mean of 7.94 (±0.03) pmol/mol at Cape Grim, Tasmania (41° S, 145° E). This is in accord with the simulation. The surface mixing ratios of CH$_3$Br displayed in Fig. 17 also show a distinct north-south gradient. These measurements are all taken in coastal regions, thus a distinct influence of the tidal forcing on bromocarbon emissions (due to algae falling dry during low tide) is likely.
20   Montzka et al. (2003) observed a decrease of methyl bromide since 1998 on the basis of ten globally distributed baseline stations. From their measurements a decrease of the methyl bromide mixing ratios from ≈10.5 pmol/mol for 1998 to 9 pmol/mol in 2003 can be inferred in the northern hemisphere. The mixing ratio of methyl bromide is lower in the southern hemisphere, decreasing from ≈ 8.2 pmol/mol in 1998 to ≈7 pmol/mol
25 in 2003.
    Figure 18 presents the annual average CH$_3$Br emission fluxes resulting from the tracer nudging (see Kerkweg et al. (2006b) for a description of the tracer nudging technique). The globally integrated emission fluxes as proposed by Warwick et al.

([2006a](#)) and as derived from our model simulation do not differ much (131 Gg/yr vs. 130.6 Gg/yr).

For higher altitudes only data from the aircraft campaigns PEM-West B ([Blake et al., 1997](#)), PEM-Tropics A and B ([Colman et al., 2001](#); [Blake et al., 2001](#); [Emmons et al., 2000](#)), STRAT ([Schauffler et al., 1998](#)), GABRIEL ([Gebhardt et al., 2008](#)) and CARIBIC ([Brenninkmeijer et al., 1999](#)) are available.

[Schauffler et al.](#) ([1998](#)) report an average of 9.45 pmol/mol and [Colman et al.](#) ([2001](#)) summarises measurements from the PEM-Tropics A (5 August to 6 October 1996) and PEM-Tropics B (6 March to 18 April 1999) campaigns. Mixing ratios of CH_3Br between 6.0 and 11.9 pmol/mol were observed, with averages of 8.9 pmol/mol and 8.6 pmol/mol for PEM-Tropics A and PEM-Tropics B, respectively. Figure [19](#) shows the simulated zonally averaged vertical methyl bromide distribution for the campaign periods of PEM-Tropics A and B though for the year 2000. The simulated mixing ratios compare well to the observations of [Colman et al.](#) ([2001](#)) and [Schauffler et al.](#) ([1998](#)). For a more detailed comparison Fig. [20](#) shows the vertical profiles as measured during the PEM-Tropics B campaign (red dots) and those resulting from the simulation (black lines). For the PEM-Tropics campaigns the simulation and the observations match very well. The vertical profiles for PEM-Tropics A are very similar and are not shown here.

The correspondence between simulations and observations decreases towards the north of the measurement domain. This might indicate some deficiency in the emission flux estimates for the mid-latitudes. Figure [21](#) shows the vertical profiles for PEM-West B. The mixing ratios are often underestimated by the model, while the shape of the profiles is reproduced. Part of the discrepancies may be explained by the negative CH_3Br trend of about 10% between 1994 (PEM-West B measurements) and 2000 due to a reduction in anthropogenic emissions ([WMO](#), [2007](#)).

However, some underestimation of the CH_3Br abundance is also apparent from the comparison with CARIBIC ([Brenninkmeijer et al.](#), [1999](#)) as well as with GABRIEL ([Gebhardt et al.](#), [2008](#)) data. Figure [22](#) displays 8 CARIBIC flights of the year 2000 and Fig. [23](#) shows the 7 GABRIEL flights, where the measurements of October 2005 are

compared to the simulation results of October 2000. The red line indicates the measurements, the black line shows the simulation results, respectively. For most flights the simulation yields too low CH_3Br mixing ratios. The methane lifetime in our simulation is 7.8 years. This is slightly lower as by Jöckel et al. (2006) (8.02 years) and well within the range of other models (8.67±1.32) (Stevenson et al., 2006). Thus chemistry is not the reason for the low CH_3Br mixing ratios. They are most likely a consequence of a still underestimated methyl bromide source. We recall that also the assumptions about the surface mixing ratios of CH_3Br to which surface CH_3Br is relaxed by TNUDGE are rather crude, i.e. because of the data paucity only latutidinal averages of surface CH_3Br mixing ratios are used. This is probably most relevant for the GABRIEL campaign as CH_3Br emissions of the tropical rainforest are not explicitly taken into account in our emission inventories. The derived lifetime of CH_3Br of about a year (Table 2), is up to a factor of two larger than previous estimates (WMO, 2007), This helps to reduce an imbalance between estimated sources and sinks (Reeves, 2003). One consequence is that substantially more CH_3Br may enter the stratosphere and contribute to ozone loss, both presently and in the natural pre-industrial atmosphere, than previously assumed.

4 Bromocarbons as sources of reactive bromine

Subsequently to the evaluation of the individual bromocarbon distributions we focus on the production of reactive bromine by photolysis of bromocarbons and their reactions with OH and the relative importance of the two pathways. In the following, the term "organic bromine" denominates the bromine contained in all six previously investigated compounds and in the halons CF_2BrCl and CF_3Br. "Reactive bromine" refers to bromine found in all gaseous compounds which are not organic bromine.

Table 3 lists the stratospheric and tropospheric global production in g(Br)/s of Br radicals by photolysis of bromocarbons and reaction with OH, respectively. The degradation of bromocarbons is by far larger in the troposphere with a total production of Br radicals of 22.08 g(Br)/s than in the stratosphere. Reaction with OH amounts

A. Kerkweg et al.

to 5.9 g(Br)/s, i.e. slightly more than one third of the total amount. Conversely, this means that photolysis is the dominant source process accounting for approximately two thirds of the bromine radical production from organic bromine. The stratospheric source is much smaller producing just as large as 0.44 g(Br)/s. Nevertheless, photolysis of CH_3Br, CH_2Br_2 and CH_2ClBr is more efficient in the stratosphere than in the troposphere. This is also illustrated by Fig. 24. In accordance with most stratospheric chemistry models (e.g. Steil et al. (1998); Teyssèdre et al. (2007)), which usually take only methyl bromide into account, CH_3Br is indeed a major stratospheric source of reactive bromine. Nevertheless, Table 3 includes a contribution from stratospheric bromoform photolysis of 0.211 g(Br)/s, which is $\approx$2.5 times higher than from methyl bromide (0.064 g(Br)/s) in the stratosphere. There might be two reasons for this surprisingly high number: First, as discussed at the end of Sect. 3.1, the simulated amount of bromoform is too high in the tropopause region leading to an overestimation of the production of Br radicals by the photolysis of bromoform. Second, the analysis shown in Table 3 was performed using the tropopause height being online diagnosed by the model. If a fixed height of 100 hPa (instead of the tropopause) would be assumed as a threshhold, the stratospheric source by photolysis of bromoform is only 0.063 g(Br)/s. Thus production of bromine radicals by photolysis of bromoform is a large bromine source in the lowermost stratosphere, but its importance decreases rapidly with altitude. In contrast, the importance of methyl bromide photolysis reaches its maximum at much higher altitudes. This is also illustrated in Fig. 24. Stratospheric bromine chemistry becomes important above the altitude where stratospheric production of bromine radicals by photolysis of bromoform has decreased to a neglible amount. Hence, our simulation does not contradict the assumption that methyl bromide is the only important bromocarbon for stratospheric chemistry as is often used for stratospheric chemistry simulations.

Even though CH_3Br is the largest organic bromine source in the stratosphere, most of it reacts with OH in the troposphere, yielding 2.2 g(Br)/s. This also holds for the two bromocarbons (CH_2Br_2 and CH_2ClBr), whose photolysis is also more efficient in

the stratosphere than in the troposphere. The sink by reaction with OH in the tro-posphere amounts for CH_2Br_2 and CH_2ClBr to 2.588 and 0.123 g(Br)/s, respectively. The largest loss for the other three bromocarbons ($CHBr_3$, $CHCl_2Br$ and $CHClBr_2$) oc-curs through photolysis in the troposphere. Reaction with OH in the stratosphere is negligibly small compared to the other production terms. However, the largest source species for bromine radicals in the troposphere is bromoform. The reason for this is twofold. First, bromoform emissions are highest and second, each molecule decom-position yields three bromine radicals. Figure 25 shows the production rate of bromine radicals by photolysis (left) of all bromine containing carbons (including halons) and by reaction with OH (middle), respectively. The right panel gives the fractional contribu-tion of photolysis to the overall (photolysis + reaction with OH) Br production. These distributions are rather similar. As the sources of bromocarbons are largest in the trop-ics, the maximum production takes place in the tropics. In contrast to the reaction of bromocarbons with OH, of which the importance decreases with height, production by photolysis reaches a second relative maximum above 100 hPa which is due to photol-ysis of methyl bromide and the halons (which are not analysed in detail here). From the right panel of Fig. 25 it is apparent that photolysis dominates as a source process throughout the atmosphere. The only regions where reaction with OH seems to be-come important are the polar regions. However, since both processes are dependent on sunlight, this is in fact a ratio of two very small terms resulting in a large uncer-tainty. Thus the relative contribution of the reaction with OH to the decomposition of the bromocarbons is highest in the boundary layer.

In summary, photolysis and reaction with OH are both important decomposition pro-cesses of bromocarbons in the troposphere although photolysis dominates, especially above the boundary layer. In the stratosphere the photolysis of halons contributes substantially to the Br production.

5   Conclusions

In this part of a series of articles, focussing on atmospheric bromine chemistry, we investigate the distribution of bromocarbons as simulated with the AC-GCM ECHAM5/MESSy. The applied emission fields follow the estimates of Warwick et al. (2006a), more specifically emission scenario 5. Depending on the bromocarbon species, the model tends to slightly under- or overestimate the abundance. For bromoform the observed (PEM) increase from the free troposphere towards the surface is very well reproduced. The model predicts an increase towards higher altitudes while the observations indicate a decrease. The CH_2Br_2 mixing ratios are overestimated by the simulation for most PEM profiles. Nevertheless, the simulated profile shape, especially the observed increase in the mixing ratio towards the surface is reproduced by the simulation. Compared to the CARIBIC data the CH_2Br_2 mixing ratios are somewhat overestimated.

The simulated CH_2ClBr mixing ratios are generally too low compared to PEM observations. On the other hand the simulated $CHClBr_2$ mixing ratios are in agreement with the measurements (PEM), while the simulated $CHCl_2Br$ mixing ratios are slightly underestimated compared to PEM-B data and partly overestimated for PEM-A.

Bromoform is too high in our simulation compared to the measurements. We conclude that this is a consequence of the overestimated emission flux, as we applied the relatively high emission scenario proposed by Warwick et al. (2006b).

The simulated methyl bromide profiles match the observations very well in the tropics, whereas this agreement decreases somewhat towards the north. This is most probably a result of the simplifying assumptions about the surface mixing ratios of CH_3Br used for the tracer nudging. The comparison with CARIBIC and GABRIEL data shows an underestimation for the same reason. Despite this underestimation our results indicate a $\approx 50\%$ longer CH_3Br lifetime than previously thought, implying a larger contribution to stratospheric ozone loss.

In summary, many bromocarbon mixing ratios are slightly overestimated by the

model. However, as the measurements are mostly within the uncertainty of the simulation, we conclude that the agreement is relatively good while the shape of the vertical profiles and the total mixing ratios are realistically reproduced except the overestimations in the UTLS for $CHBr_3$ and CH_2Br_2 .

Based on the evaluated bromocarbon distributions the production processes of reactive bromine were investigated. Photolysis was found to be the dominant decomposition process in the stratosphere for all bromocarbons. In the troposphere reaction with OH is the dominant loss process for CH_3Br, CH_2Br_2 and CH_2ClBr, whereas photolysis is most important for $CHBr_3$, $CHCl_2Br$ and $CHClBr_2$.

This analysis focussed on the bromine source from bromocarbons. In Part-III of this series we will investigate the importance of bromine release from sea salt aerosol.

References

Andreae, M., Atlas, E., Harris, G., Helas, G., deKock, A., Koppmann, R., Maenhaut, W., Mano, S., Pollock, W., Rudolph, J., Scharffe, D., Schebeske, G., and Welling, M.: Methyl halide emissions from savanna fires in southern Africa, J. Geophys. Res., 101, 23 603–23 613, 1996. 9490

Blake, N., Blake, D., Chen, T., Collins, J., Sachse, G., Anderson, B., and Rowland, F.: Distribution and seasonality of selected hydrocarbons and halocarbons over the western Pacific basin during PEM-West A and PEM-West B, J. Geophys. Res., 102, 28 315–28 331, 1997. 9491

Blake, N., Blake, D., Simpson, I., Lopez, J., Johnston, N., Swanson, A., Katzenstein, A., Meinardi, S., Sive, B., Colman, J., Atlas, E., Flocke, F., Vay, S., Avery, M., and Rowland, F.: Large-scale latitudinal and vertical distributions of NMHCs and selected halocarbons in

Part 2: Sources of reactive bromine – Bromocarbons

A. Kerkweg et al.

|◄ | ►|

◄ | ►

Back | Close

Full Screen / Esc

Printer-friendly Version

Interactive Discussion

the troposphere over the Pacific Ocean during the March–April 1999 Pacific Exploratory Mission (PEM-Tropics B), J. Geophys. Res., 106, 32 627–32 644, 2001. 9484, 9489, 9491

Brenninkmeijer, C., Crutzen, P., Fischer, H., Gusten, H., Hans, W., Heinrich, G., Heintzenberg, J., Hermann, M., Immelmann, T., Kersting, D., Maiss, M., Nolle, M., Pitscheider, A., Pohlkamp, H., Scharffe, D., Specht, K., and Wiedensohler, A.: CARIBIC – Civil aircraft for global measurement of trace gases and aerosols in the tropopause region, J. Atmos. Oc. Tech., 16, 1373–1383, 1999. 9480, 9486, 9491

Carpenter, L. and Liss, P.: On temperate sources of bromoform and other reactive organic bromine gases, J. Geophys. Res., 105, 20 539–20 547, 2000. 9483

Carpenter, L., Sturges, W., Penkett, S., Liss, P., Alicke, B., Hebestreit, K., and Platt, U.: Short-lived alkyl iodides and bromides at Mace Head, Ireland: Links to biogenic sources and halogen oxide production, J. Geophys. Res., 104, 1679–1689, 1999. 9483, 9488, 9490

Carpenter, L., Wevill, D., O'Doherty, S., Spain, G., and Simmonds, P.: Atmospheric bromoform at Mace Head, Ireland: seasonality and evidence for a peatland source, Atmos. Chem. Phys., 5, 2927–2934, 2005,
http://www.atmos-chem-phys.net/5/2927/2005/. 9483

Carpenter, L. J., Liss, P. S., and Penkett, S. A.: Marine organohalogens in the atmosphere over the Atlantic and Southern Oceans, J. Geophys. Res., doi:10.1029/2002JD002769, 2003. 9483, 9486

Colman, J., Swanson, A., Meinardi, S., Sive, B., Blake, D., and Rowland, F.: Description of the analysis of a wide range of volatile organic compounds in whole air samples collected during PEM-Tropics A and B, Anal. Chem., 73, 3723–3731, 2001. 9484, 9486, 9489, 9491

Emmons, L. K., Hauglustaine, D. A., Müller, J.-F., Carroll, M. A., Brasseur, G. P., Brunner, D., Staehelin, J., Thouret, V., and Marenco, A.: Data composites of airborne observation of tropospheric ozone and its precursor, J. Geophys. Res., 105, 20 497–20 538, 2000. 9484, 9489, 9491

Gebhardt, S., Colomb, A., Hofmann, R., Williams, J., and Lelieveld, J.: Halogenated organic species over the tropical rainforest, Atmos. Chem. Phys. Discuss., 8, 1159–1190, 2008,
http://www.atmos-chem-phys-discuss.net/8/1159/2008/. 9491

Giorgetta, M. A., Manzini, E., and Roeckner, E.: Forcing of the quasi-biennial oscillation from a broad spectrum of atmospheric waves, Geophys. Res. Lett., 29, doi:10.1029/2002GL014756, 2002. 9480

Giorgetta, M. A., Manzini, E., Roeckner, E., Esch, M., and Bengtson, L.: Climatology and

Title Page

Abstract | Introduction

Conclusions | References

Tables | Figures

◄ | ►►

◄ | ►

Back | Close

Full Screen / Esc

Printer-friendly Version

Interactive Discussion

forcing of the quasi-biennial oscillation in the MAECHAM5 model, J. Clim., 19, 3882–3901, 2006. 9480

Gros, V., Williams, J., van Aardenne, J., Salisbury, G., Hofmann, R., Lawrence, M., von Kuhlmann, R., Lelieveld, J., Krol, M., Berresheim, H., Lobert, J., and Atlas, E.: Origin of anthropogenic hydrocarbons and halocarbons measured in the summertime european out-flow (on Crete in 2001), Atmos. Chem. Phys., 3, 1223–1235, 2003, http://www.atmos-chem-phys.net/3/1223/2003/. 9490

Hoell, J. M., Davis, D. D., Liu, S. C., Newell, R. E., Akimoto, H., McNeal, R. J., and Bendura, R. J.: The Pacific Exploratory Mission-West Phase B: February-March 1994, J. Geophys. Res., 102, 28 223–28 239, 1997. 9480

Hoell, J. M., Davis, D. D., Jacob, D. J., Rodgers, M. O., Newell, R. E., Fuelberg, H. E., McNeal, R. J., Raper, J. L., and Bendura, R. J.: Pacific Exploratory Mission in the tropical Pacific: PEM-Tropics A, August-September 1996, J. Geophys. Res., 104, 5567–5583, 1999. 9480

Jöckel, P., Sander, R., Kerkweg, A., Tost, H., and Lelieveld, J.: Technical Note: The Modular Earth Submodel System (MESSy) - a new approach towards Earth System Modeling, Atmos. Chem. Phys., 5, 433–444, 2005, http://www.atmos-chem-phys.net/5/433/2005/. 9480

Jöckel, P., Tost, H., Pozzer, A., Brühl, C., Buchholz, J., Ganzeveld, L., Hoor, P., Kerk-weg, A., Lawrence, M. G., Sander, R., Steil, B., Stiller, G., Tanarhte, M., Taraborrelli, D., van Aardenne, J., and Lelieveld, J.: The atmospheric chemistry general circulation model ECHAM5/MESSy1: Consistent simulation of ozone from the surface to the mesosphere, Atmos. Chem. Phys., 6, 5067–5104, 2006, http://www.atmos-chem-phys.net/6/5067/2006/. 9480, 9481, 9492

Kerkweg, A., Buchholz, J., Ganzeveld, L., Pozzer, A., Tost, H., and Jöckel, P.: Technical Note: an implementation of the dry removal processes DRY DEPosition and SEDImentation in the Modular Earth Submodel System (MESSy), Atmos. Chem. Phys., 6, 4617–4632, 2006s, http://www.atmos-chem-phys.net/6/4617/2006/. 9481

Kerkweg, A., Sander, R., Tost, H., and Jöckel, P.: Technical Note: Implementation of prescribed (OFFLEM), calculated (ONLEM), and pseudo-emissions (TNUDGE) of chemical species in the Modular Earth Submodel System (MESSy), Atmos. Chem. Phys., 6, 3603–3609, 2006b, http://www.atmos-chem-phys.net/6/3603/2006/. 9481, 9490

Kerkweg, A., Sander, R., Tost, H., Jöckel, P., and Lelieveld, J.: Technical Note: simulation of detailed aerosol chemistry on the global scale using MECCA-AERO, Atmos. Chem. Phys.,

Part 2: Sources of reactive bromine – Bromocarbons

A. Kerkweg et al.

Title Page

Abstract | Introduction

Conclusions | References

Tables | Figures

◄ | ►

◄ | ►

Back | Close

Full Screen / Esc

Printer-friendly Version

Interactive Discussion

7, 2973–2985, 2007, http://www.atmos-chem-phys.net/7/2973/2007/. 9481, 9482

Kerkweg, A., Jöckel, P., Pozzer, A., Tost, H., Sander, R., Schulz, M., Stier, P., Vignati, E., Wilson, J., and Lelieveld, J.: Consistent simulation of bromine chemistry from the marine boundary layer to the stratosphere – Part 1: Model description, sea salt aerosols and pH, Atmos. Chem. Phys. Discuss., 8, 7217–7262, 2008 9481

Kourtidis, K., Borchers, R., and Fabian, P.: Dibromomethane (CH2Br2) measurements at the upper troposphere and lower stratosphere, Geophys. Res. Lett., 23, 2581–2583, 1996. 9487, 9513

Landgraf, J. and Crutzen, P.: An Efficient Method for Online Calculation of Photolysis and Heating Rates, J. Atmos. Sci., 55, 863–878, 1998. 9481

Lelieveld, J., Butler, T. M., Crowley, J. N., Dillon, T. J., Fischer, H., Ganzeveld, L., Harder, H., Lawrence, M. G., Martinez, M., Taraborrelli, D., and Williams, J.: Atmospheric oxidation capacity sustained by a forest, Nature, 452, 737–740, 2008. 9480

Montzka, S., Butler, J., Hall, B., Mondeel, D., and Elkins, J.: A decline in tropospheric organic bromine, Geophys. Res. Lett., 30, doi:10.1029/2003GL017745, 2003. 9490

Pozzer, A., Jöckel, P., Sander, R., William, J., Ganzeveld, L., and Lelieveld, J.: Technical Note: The MESSy-submodel AIRSEA calculating the air-sea exchange of chemical species, Atmos. Chem. Phys., 6, 5435–5444, 2006, http://www.atmos-chem-phys.net/6/5435/2006/. 9481

Prinn, R. G., Weiss, R. F., Fraser, P. J., Simmonds, P. G., Cunnold, D. M., Alyea, F. N., O'Doherty, S., Salameh, P., Miller, B. R., Huang, J., Wang, R. H. J., Hartley, D. E., Harth, C., Steele, L. P., Sturrock, G., Midgley, P. M., and McCulloch, A.: A history of chemically and radiatively important gases in air deduced from ALE/GAGE/AGAGE, J. Geophys. Res., 105, 17 751–17 792, 2000. 9482

Ramacher, B., Rudolph, J., and Koppmann, R.: Hydrocarbon measurements during tropospheric ozone depletion events: Evidence for halogen atom chemistry, J. Geophys. Res., 104, 3633–3653, 1999. 9483, 9485, 9490

Raper, J. L., Kleb, M. M., Jacob, D. J., Davis, D. D., Newell, R. E., Fuelberg, H. E., Bendura, R. J., Hoell, J. M., and McNeal, R. J.: Pacific Exploratory Mission in the Tropical Pacific: PEM-Tropics B, March-April 1999, J. Geophys. Res., 106, 32 401–32 425, 2001. 9480

Reeves, C.: Atmospheric budget implications of the temporal and spatial trends in methyl bromide concentration, J. Geophys. Res., 108, doi:10.1029/2002JD002943, 2003. 9492

Part 2: Sources of reactive bromine – Bromocarbons

A. Kerkweg et al.

Title Page

Abstract	Introduction
Conclusions	References
Tables	Figures

|◄|►|
|◄|►|

Back | Close

Full Screen / Esc

Printer-friendly Version

Interactive Discussion

Roeckner, E., Bäuml, G., Bonaventura, L., Brokopf, R., Esch, M., Giorgetta, M., Hagemann, S., Kirchner, I., Kornblueh, L., Manzini, E., Rhodin, A., Schlese, U., Schulzweida, U., and Tompkins, A.: The atmospheric general circulation model ECHAM5, Tech. rep., Max Planck-Institute for Meteorology, 2003. 9480

5   Roeckner, E., Brokopf, R., Esch, M., Giorgetta, M., Hagemann, S., Kornblueh, L., Manzini, E., Schlese, U., and Schulzweida, U.: The atmospheric general circulation model ECHAM5. PART II: Sensitivity of Simulated Climate to Horizontal and Vertical Resolution, Tech. Rep. MPI-Report 354, Max Planck-Institute for Meteorology, http://www.mpimet.mpg.de/fileadmin/ publikationen/Reports/max_scirep_354.pdf, 2004. 9480

10   Roeckner, E., Brokopf, R., Esch, M., Giorgetta, M., Hagemann, S., Kornblueh, L., Manzini, E., Schlese, U., and Schulzweida, U.: Sensitivity of simulated climate to horizontal and vertical resolution in the ECHAM5 atmosphere model, J. Clim., 19, 3771–3791, 2006. 9480

Sander, R., Kerkweg, A., Jöckel, P., and Lelieveld, J.: Technical Note: The new comprehensive atmospheric chemistry module MECCA, Atmos. Chem. Phys., 5, 445–450, 2005,

15   http://www.atmos-chem-phys.net/5/445/2005/. 9481, 9482

Sander, S. P., Finlayson-Pitts, B. J., Friedl, R. R., Golden, D. M., Huie, R. E., Kolb, C. E., Kurylo, M. J., Molina, M. J., Moortgat, G. K., Orkin, V. L., and Ravishankara, A. R.: Chemical Kinetics and Photochemical Data for Use in Atmospheric Studies, Evaluation Number 14, JPL Publication 02-25, Jet Propulsion Laboratory, Pasadena, CA, 2003. 9482

20   Schall, C. and Heumann, K. G.: GC determination of volatile organoiodine and organobromine compounds in Arctic seawater and air samples, Fresenius J. Anal. Chem., 346, 717–722, 1993. 9488

Schauffler, S., Heidt, L., Pollock, W. H., Gilpin, T., Vedder, J., solomon, S., Lueb, R., and Atlas, E.: Measurements of halogenated organic compounds near the tropical tropopause,

25   Geophys. Res. Lett., 20, 2567–2570, 1993. 9487

Schauffler, S., Atlas, E., Flocke, F., Lueb, R., Stroud, V., and Travnicek, W.: Measurements of bromine containing organic compounds at the tropical tropopause, Geophys. Res. Lett., 25, 317–320, 1998. 9484, 9488, 9489, 9491

Simmonds, P., Derwent, R., Manning, A., Fraser, P., Krummel, P., O'Doherty, S., Prinn, R.,

30   Cunnold, D., Miller, B., Wang, H., Ryall, D., Porter, L., Weiss, R., and Salameh, P.: AGAGE observations of methyl bromide and methyl chloride at Mace Head, Ireland, and Cape Grim, Tasmania, 1998-2001, J. Atmos. Chem., 47, 243–269, 2004. 9490

Steil, B., Dameris, M., Brühl, C., Crutzen, P., Grewe, V., Ponater, M., and Sausen, R.: De-

Title Page

Abstract | Introduction

Conclusions | References

Tables | Figures

|◄ | ►|

◄ | ►

Back | Close

Full Screen / Esc

Printer-friendly Version

Interactive Discussion

velopment of a chemistry module for GCMs: first results of a multiannual integration, Ann. Geophys., 16, 205–228, 1998, http://www.ann-geophys.net/16/205/1998/. 9493

Stevenson, D., Dentener, F., Schultz, M., Ellingsen, K., van Noije, T., Wild, O., Zeng, G., Amann, M., Atherton, C., Bell, N., Bergmann, D., Bey, I., Butler, T., Cofala, J., Collins, W., Derwent, R., Doherty, R., Drevet, J., Eskes, H., Fiore, A., Gauss, M., Hauglustaine, D., Horowitz, L., Isaksen, I., Krol, M., Lamarque, J., Lawrence, M., Montanaro, V., Muller, J., Pitari, G., Prather, M., Pyle, J., Rast, S., Rodriguez, J., Sanderson, M., Savage, N., Shindell, D., Strahan, S., Sudo, K., and Szopa, S.: Multimodel ensemble simulations of present-day and near-future tropospheric ozone, J. Geophys. Res., 111, doi:10.1029/2005JD006338, 2006. 9492

Stickler, A., Fischer, H., Bozem, H., Gurk, C., Schiller, C., Martinez-Harder, M., Kubistin, D., Harder, H., Williams, J., Eerdekens, G., Yassaa, N., Ganzeveld, L., Sander, R., and Lelieveld, J.: Chemistry, transport and dry deposition of trace gases in the boundary layer over the tropical Atlantic Ocean and the Guyanas during the GABRIEL field campaign, Atmos. Chem. Phys., 7, 3933–3956, 2007, http://www.atmos-chem-phys.net/7/3933/2007/. 9480

Teyssèdre, H., Michou, M., Clark, H. L., Josse, B., Karcher, F., Olivié, D., Peuch, V.-H., Saint-Martin, D., Cariolle, D., Attié, J.-L., Nédélec, P., Ricaud, P., Thouret, V., van der A, R. J., Volz-Thomas, A., and Chéroux, F.: A new tropospheric and stratospheric Chemistry and Transport Model MOCAGE-Climat for multi-year studies: evaluation of the present-day climatology and sensitivity to surface processes, Atmos. Chem. Phys., 7, 5815–5860, 2007, http://www.atmos-chem-phys.net/7/5815/2007/. 9493

Tost, H., Jöckel, P., Kerkweg, A., Sander, R., and Lelieveld, J.: Technical note: A new comprehensive SCAVenging submodel for global atmospheric chemistry modelling, Atmos. Chem. Phys., 6, 565–574, 2006a, http://www.atmos-chem-phys.net/6/565/2006/. 9480

Tost, H., Jöckel, P., and Lelieveld, J.: Influence of different convection parameterisations in a GCM, Atmos. Chem. Phys., 6, 5475–5493, 2006b, http://www.atmos-chem-phys.net/6/5475/2006/. 9480, 9485

Tost, H., Jöckel, P., Kerkweg, A., Pozzer, A., Sander, R., and Lelieveld, J.: Global cloud and precipitation chemistry and wet deposition: tropospheric model simulations with ECHAM5/MESSy1, Atmos. Chem. Phys., 7, 2733–2757, 2007a, http://www.atmos-chem-phys.net/7/2733/2007/. 9481

Title Page

Abstract | Introduction

Conclusions | References

Tables | Figures

|◄ | ►|

◄ | ►

Back | Close

Full Screen / Esc

Printer-friendly Version

Interactive Discussion

Tost, H., Jöckel, P., and Lelieveld, J.: Lightning and convection parameterisations – uncertainties in global modelling, Atmos. Chem. Phys., 4553–4568, 2007b. 9480

Vignati, E., Wilson, J., and Stier, P.: M7: An efficient size-resolved aerosol microphysics module for large-scale aerosol transport, J. Geophys. Res., 109, D22202, doi: 10.1029/2003JD004486, 2004. 9481

Warwick, N., Pyle, J., Carver, G., Yang, X., Savage, N., O'Connor, F., and Cox, R.: Global modeling of biogenic bromocarbons, J. Geophys. Res., 111, doi:10.1029/2006JD007264, 2006a. 9479, 9481, 9488, 9490, 9495, 9504

Warwick, N., Pyle, J., and Shallcross, D.: Global modelling of the Atmospheric Methyl Bromide Budget, J. Atmos. Chem., 54, 133–159, doi:10.1007/s10874-006-9020-3, 2006b. 9479, 9484, 9495

Wesely, M.: Parameterization of the surface resistances to gaseous dry depposition in regional-scale numerical models, Atmos. Environ., 23, 1293–1304, 1989. 9481

WMO, ed.: Scientific Assessment of Ozone Depletion: 2006, chap. Global ozone monitoring and research project, p. 572 pp., Report No. 50, World Meteorological Organization, Geneva, Schwitzerland, 2007. 9484, 9491, 9492, 9504

Yang, X., Cox, R. A., Warwick, N. J., Pyle, J. A., Carver, G. D., O'Connor, F. M., and Savage, N. H.: Tropospheric bromine chemistry and its impacts on ozone: A model study, J. Geophys. Res., 110, D23311, doi:10.1029/2005JD006244, 2005. 9479, 9482

Yokouchi, Y., Mukai, H., Yamamoto, H., Otsuki, A., Saitoh, C., and Nojiri, Y.: Distribution of methyl iodide, ethyl iodide, bromoform, and dibromomethane over the ocean (east and southeast Asian seas and the western Pacific), J. Geophys. Res., 102, 8805–8807, 1997. 9483, 9485

Table 1. This Table contains a list of all abbreviations used in this article.

abbreviation	
AASE-II	Airborne Arctic Stratospheric Expedition II
AC-GCM	Atmospheric Chemistry General Circulation Model
AIRSEA	Ms.[a]: trace gas air-sea exchange
CARIBIC	Civil Aircraft for the Regular Investigation of the atmosphere. Based on an Instrument Container
CTM	Chemical Transport Model
CLOUD	Ms.[a]: cloud microphysics
CONVECT	Ms.[a]: convection parameterisation
CVTRANS	Ms.[a]: convective transport of tracers
DRYDEP	Ms.[a]: dry deposition of gases and aerosols
E5/M1[+]	extended ECHAM5/MESSy version 1
ECHAM5	atmospheric general circulation model
ECMWF	European Centre of Medium-range Weather Forecasting
GABRIEL	Guyanas Atmosphere-Biosphere exchange and Radicals Intensive Experiment with the Learjet
GCM	general circulation model
H2O	Ms.[a]: feedback control for chemical tendency of H2O
HETCHEM	Ms.[a]: heterogenous chemistry
JVAL	Ms.[a]: photolysis rates
L87	abbr. for vertical number of layers (L87 = 87 vertical layers)
LNOX	Ms.[a]: Lightning NO_x
M7	Ms.[a]: aerosol dynamical model
MAECHAM5	middle atmosphere version of ECHAM5
MBL	Marine Boundary Layer
MECCA (-AERO)	Ms.[a]: gas and aerosol phase chemistry
MESSy	Modular Earth Submodel System
MINOS	Mediterranean Intensive Oxidant Study
OFFLEM	Ms.[a]: calculating offline emissions
ONLEM	Ms.[a]: calculating online emissions
PARFORCE	Particle Formation and Fate in the Coastal Environment, measurement campaign
PEM	Pacific Exploratory Mission
PSC	Ms.[a]: polar stratospheric clouds
RAD4ALL	Ms.[a]: radiation
QBO	Quasi-Biennial Oscillation (process and Ms.[a])
TOMCAT	Nowadays only a name for a CTM
SCAV	Ms.[a]: scavenging and cloud chemistry of gases and aerosol particles
SEDI	Ms.[a]: sedimentation of aerosol particles
SOAPEX	Southern Ocean Atmospheric Photochemistry EXperiment, measurement campaign
STRAT	Stratospheric Tracers of Atmospheric Transport
TROPOP	Ms.[a]: diagnostics of tropopause and boundary layer height
UTLS	upper troposphere/ lower stratosphere

Ms. [a]: refers to MESSy submodel, i.e. the abbreviation is a name of a MESSy submodel describing the respective process.

Title Page

Abstract | Introduction

Conclusions | References

Tables | Figures

|◄ | ►|

◄ | ►

Back | Close

Full Screen / Esc

Printer-friendly Version

Interactive Discussion

Table 2. Simulated annually averaged global column burdens, the annually integrated emission and dry deposition fluxes, and annually averaged lifetimes of the six bromocarbons. The emission fluxes are adopted from Warwick et al. (2006a), scenario 5. The WMO lifetimes are taken from WMO (2007).

species	burden Gg	emission Gg/yr	dry deposition Gg/yr	life time days	WMO lifetime days
CH_3Br	136.1	130.6	46.1	386	255
$CHBr_3$	33.2	595.0	30.2	20	26
CH_2Br_2	31.0	113.0	12.1	100	120
CH_2ClBr	2.8	6.8	1.0	150	150
$CHCl_2Br$	2.1	16.0	0.7	48	78
$CHClBr_2$	2.3	23.0	1.1	36.5	69

Table 3. Production of Br by photolysis (hν) and reaction with OH in g/s in the stratosphere (strat) and troposphere (trop), respectively.

species	hν		OH	
	strat	trop	strat	trop
CH_3Br	0.064	0.003	0.031	2.201
$CHBr_3$	0.211	15.804	0.003	0.713
CH_2Br_2	0.022	0.006	0.043	2.588
CH_2ClBr	0.002	<0.001	0.003	0.123
$CHCl_2Br$	0.003	0.124	<0.001	0.102
$CHClBr_2$	0.007	0.332	<0.001	0.183
total	0.361	16.27	0.082	5.909
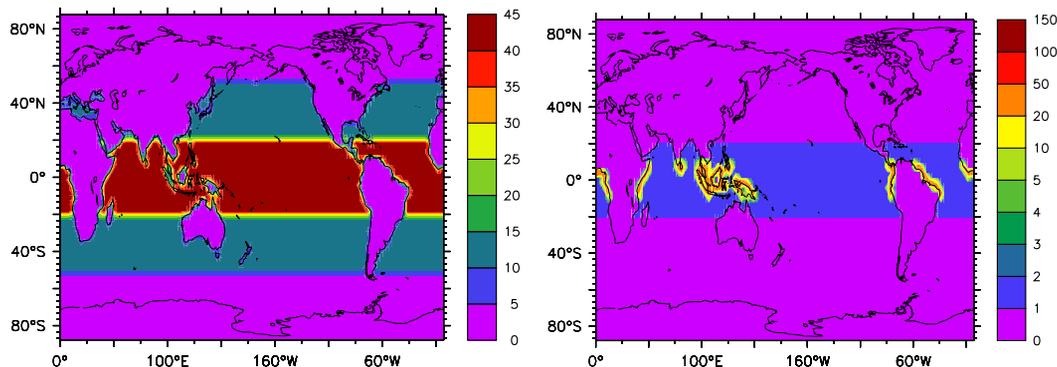
Fig. 1. Simulated annually integrated bromocarbon emission fluxes for CH_2ClBr (left $\mu g/(m^2 yr)$) and $CHBr_3$ (right, $mg/(m^2 yr)$).
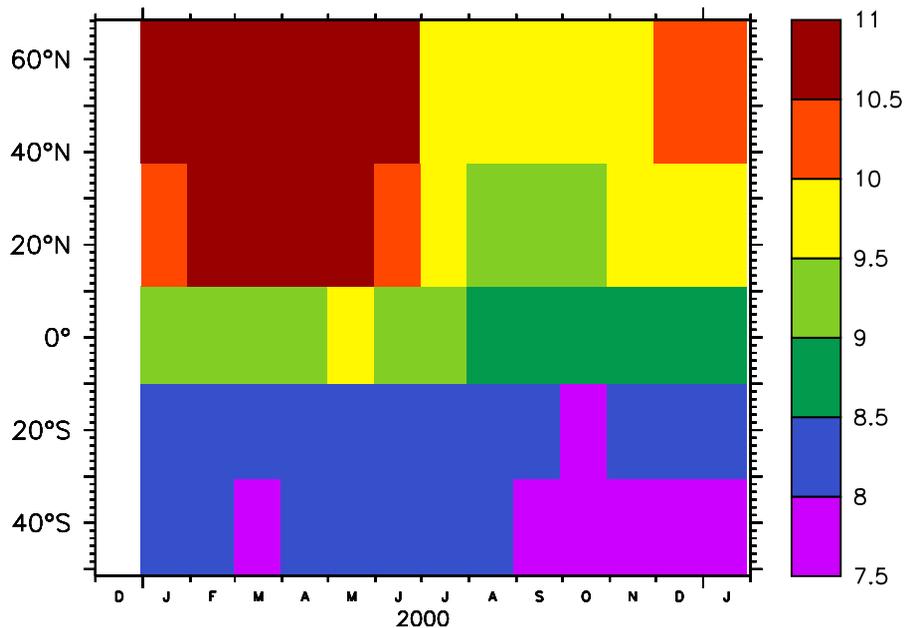
Fig. 2. Annual cycle of the surface CH$_3$Br mixing ratios (pmol/mol) as used by the submodel TNUDGE.

Title Page

Abstract | Introduction

Conclusions | References

Tables | Figures

◄◄ | ►►

◄ | ►

Back | Close

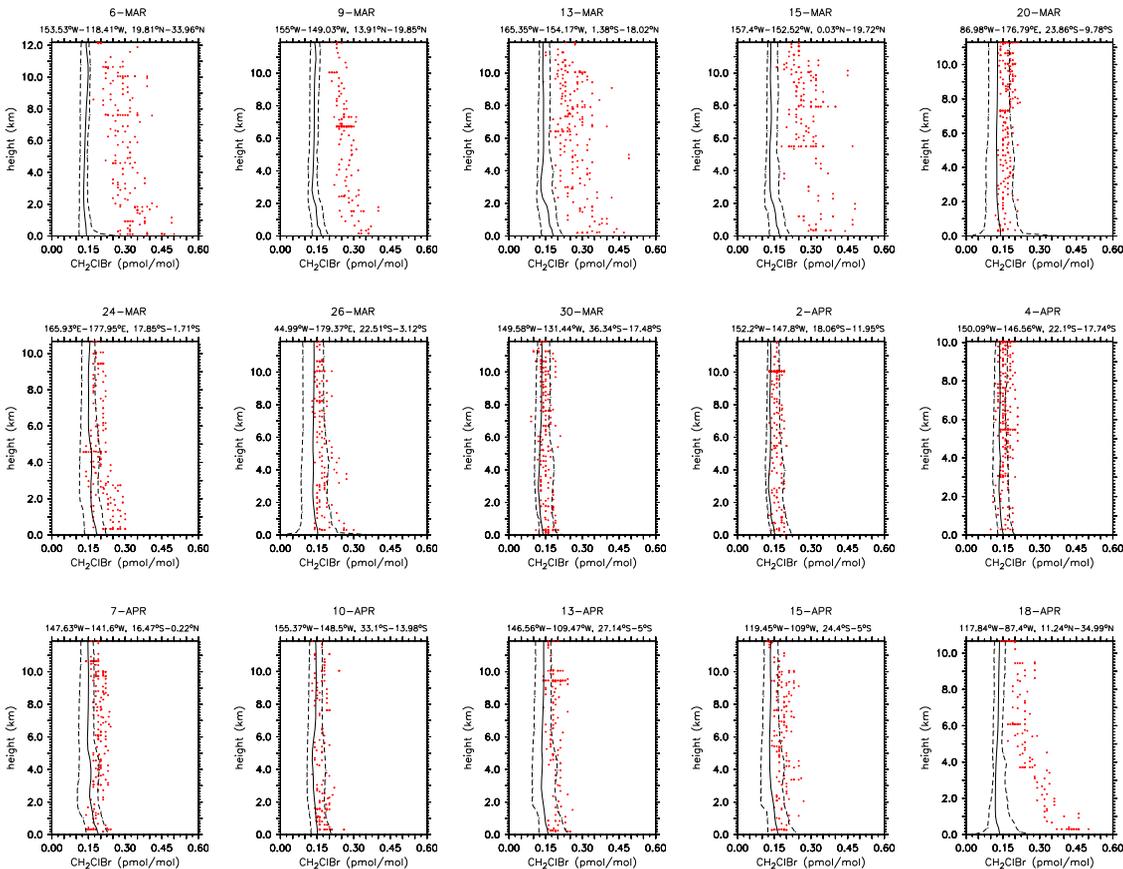Full Screen / Esc

Printer-friendly Version

Interactive Discussion
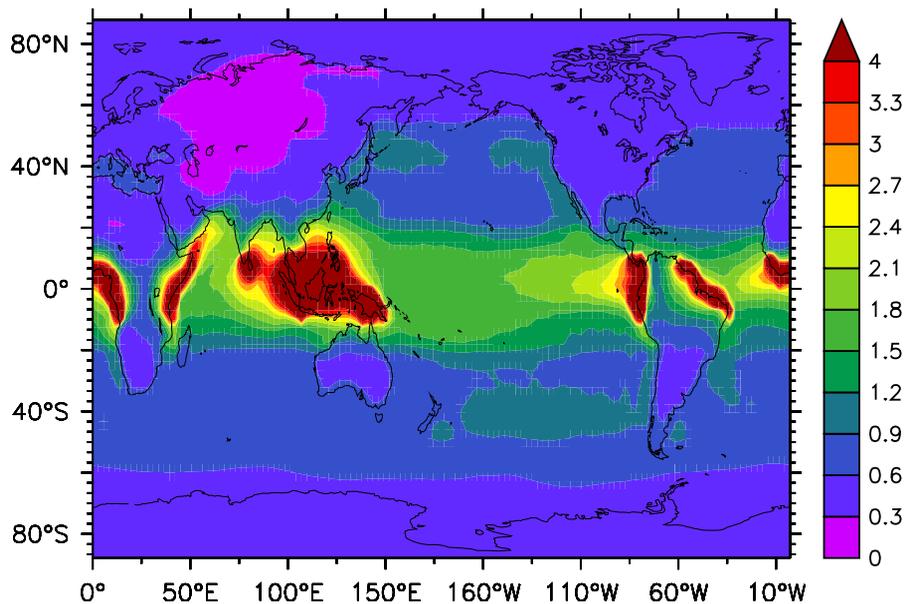
Fig. 3. Simulated annually averaged CHBr$_3$ mixing ratio (pmol/mol) in the lowermost model layer for the year 2000.
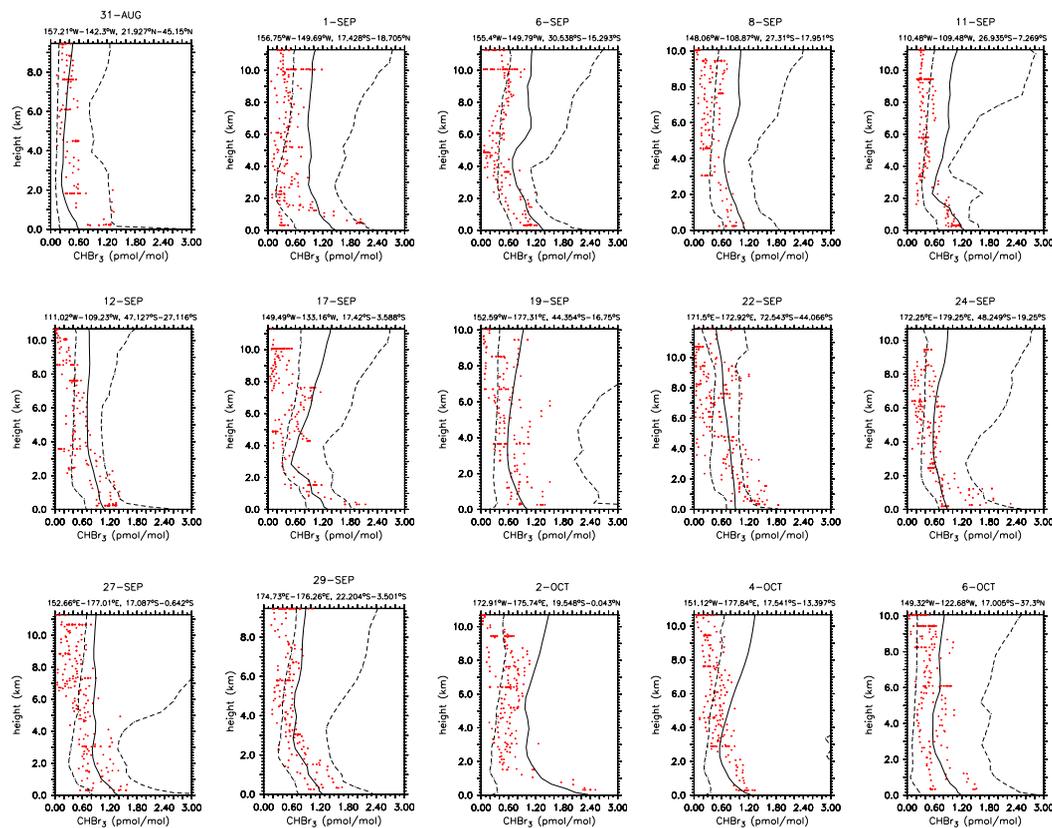
Fig. 4. CHBr$_3$ vertical profiles (pmol/mol) as measured during the PEM-Tropics-A DC8 campaign (red dots). The black lines show the simulated vertical profiles averaged over the flight period and area. The dashed lines indicate the simulated minimum and maximum CHBr$_3$ mixing ratios during the whole campaign period.
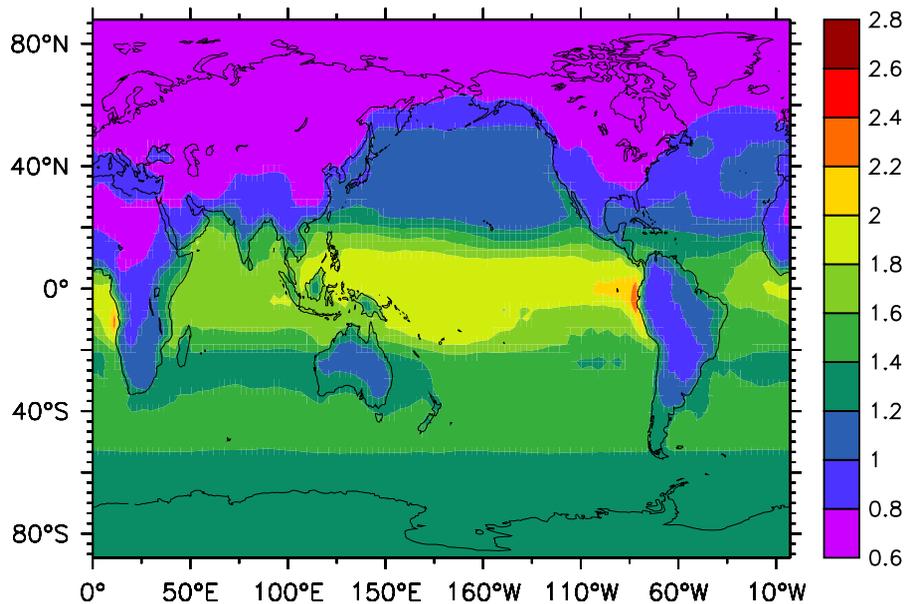
Fig. 5. Simulated annual average CH_2Br_2 in pmol/mol in the lowermost model layer.
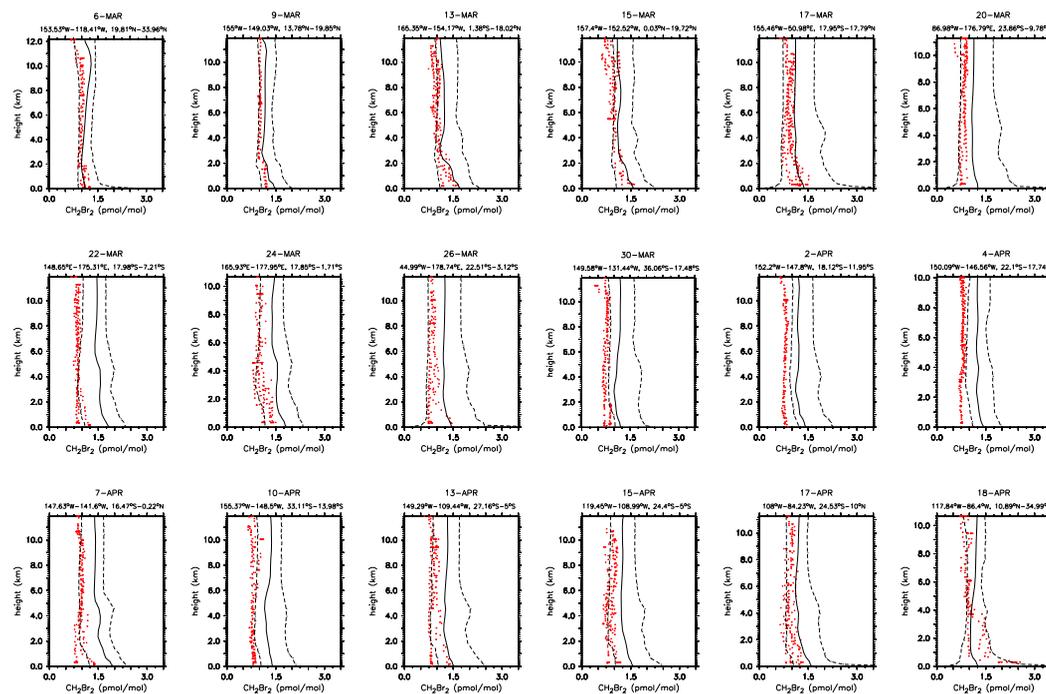
Fig. 6. As Fig. 4 but for CH$_2$Br$_2$ and the PEM-Tropics B campaign.
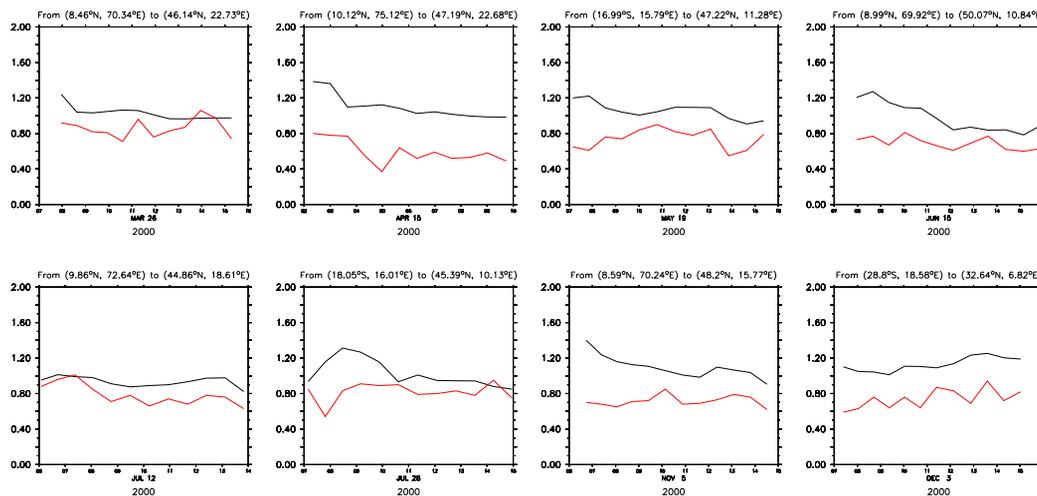
Fig. 7. Point to point comparison of CH_2Br_2 mixing ratios from the CARIBIC aircraft data (red line) and model results (black) as a function of time of day from March - December 2000.
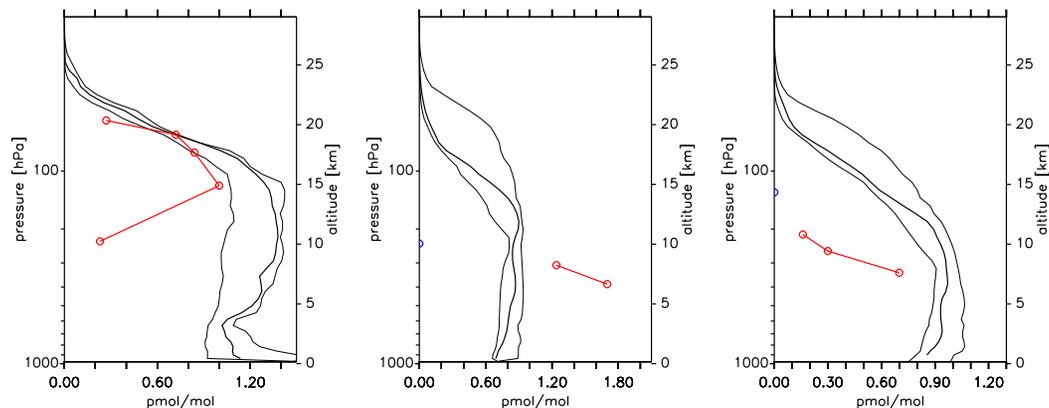
Fig. 8. CH$_2$Br$_2$ profiles in pmol/mol: Left: 9 April, Hyderabad, India; middle: 18 January, Kiruna, Sweden; right: 7 March, Kiruna, Sweden. The thick black line indicates the simulated profile. The thin black lines show the minimum and maximum simulated mixing ratios during a 14-day interval around the actual measurements. The red lines and the circles present the measurements of Kourtidis et al. (1996). The blue circles indicate measurements below the detection limit.
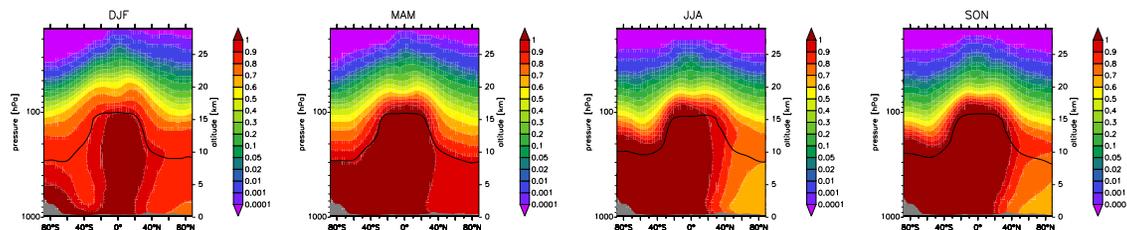
Fig. 9. Simulated vertical distribution of CH_2Br_2 in pmol/mol. Shown are seasonal averages; DJF: December 1999, January 2000, February 2000; MAM: March–May 2000; JJA: June-August 2000; SON: September–November 2000.
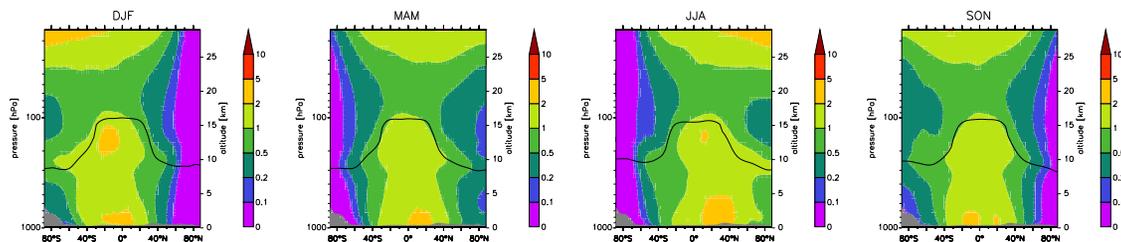
Fig. 10. Simulated vertical distribution of OH in $10^6/cm^3$. Seasons as in Fig. 9.
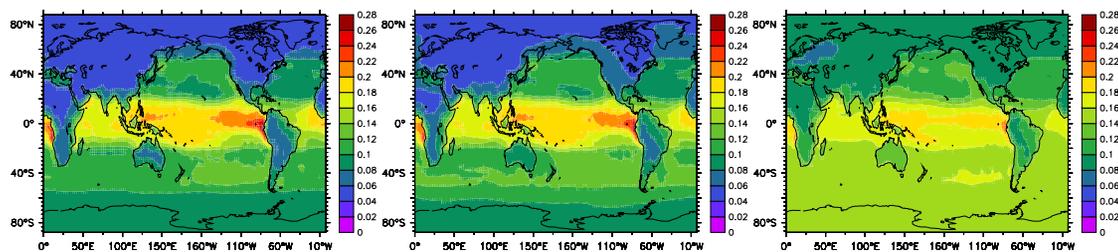
Fig. 11. Annual average CHClBr$_2$ (left), CHCl$_2$Br (middle) and CH$_2$ClBr (right) in the lowermost model layer in pmol/mol.
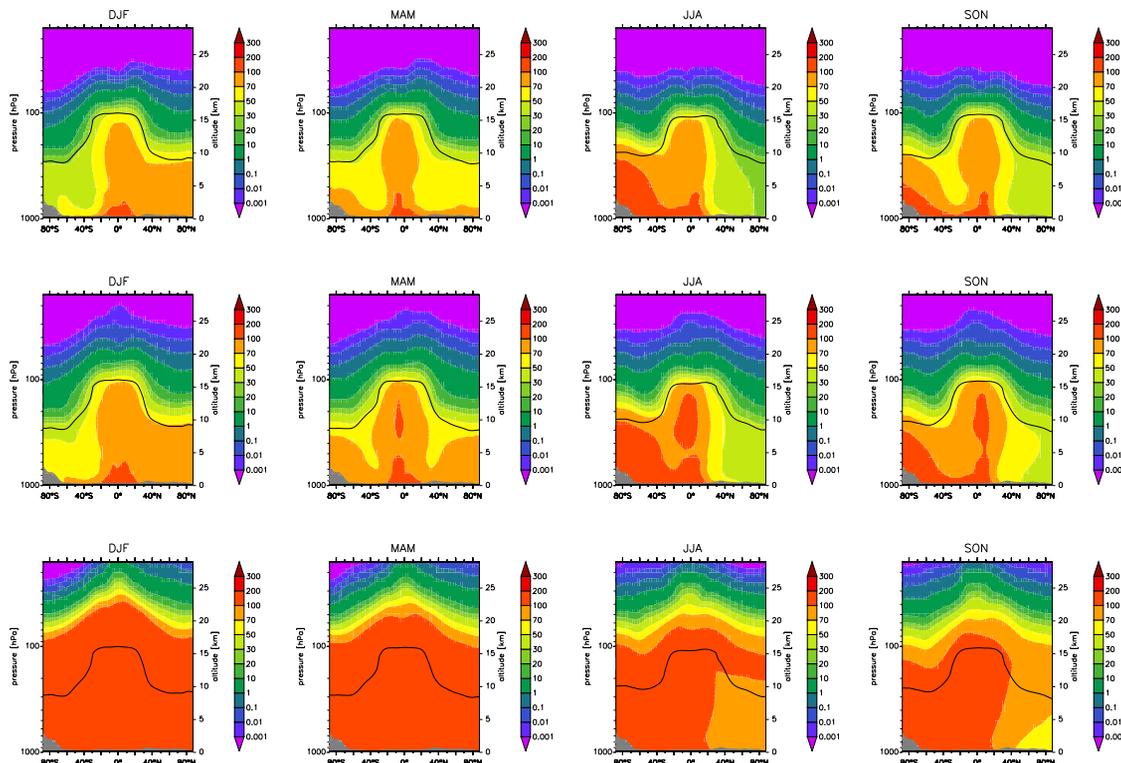
Fig. 12. Simulated vertical distribution of CHClBr$_2$ (upper row), CHCl$_2$Br (middle row) and CH$_2$ClBr (lower row) in fmol/mol. Shown are seasonal averages from left to right; DJF: December 1999–February 2000; MAM: March–May 2000; JJA: June–August 2000; SON: September–November 2000.

Full Screen / Esc

Printer-friendly Version

Interactive Discussion
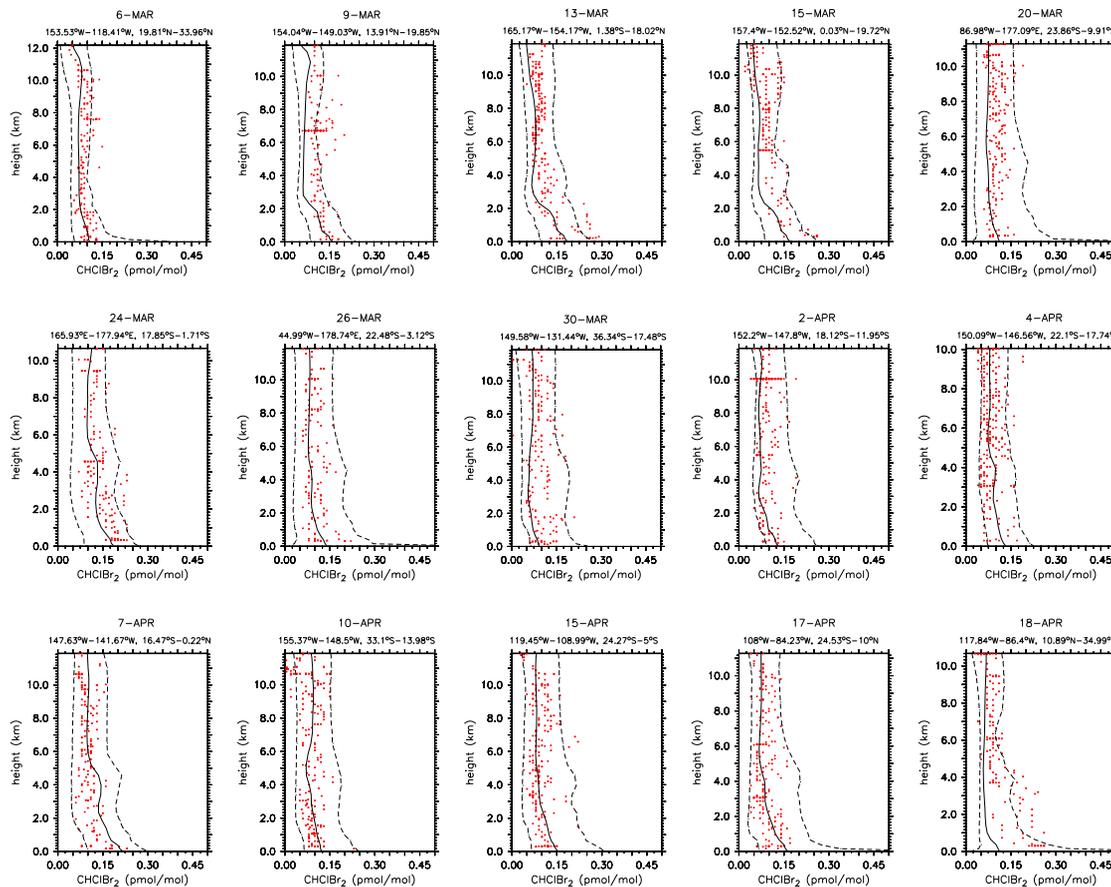
Fig. 13. As Figure 4 but for CHClBr$_2$ and the PEM-Tropics B campaign.
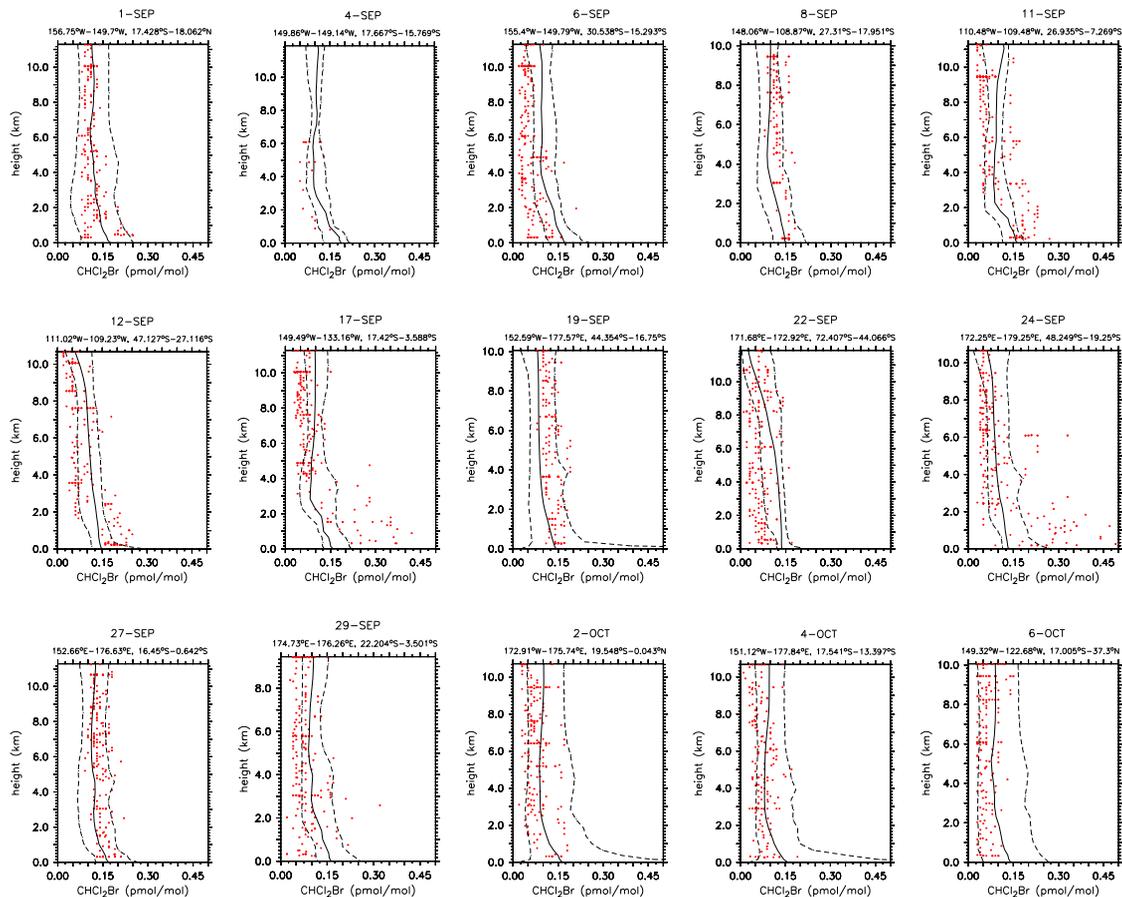
Fig. 14. As Fig. 4 but for CHCl₂Br.
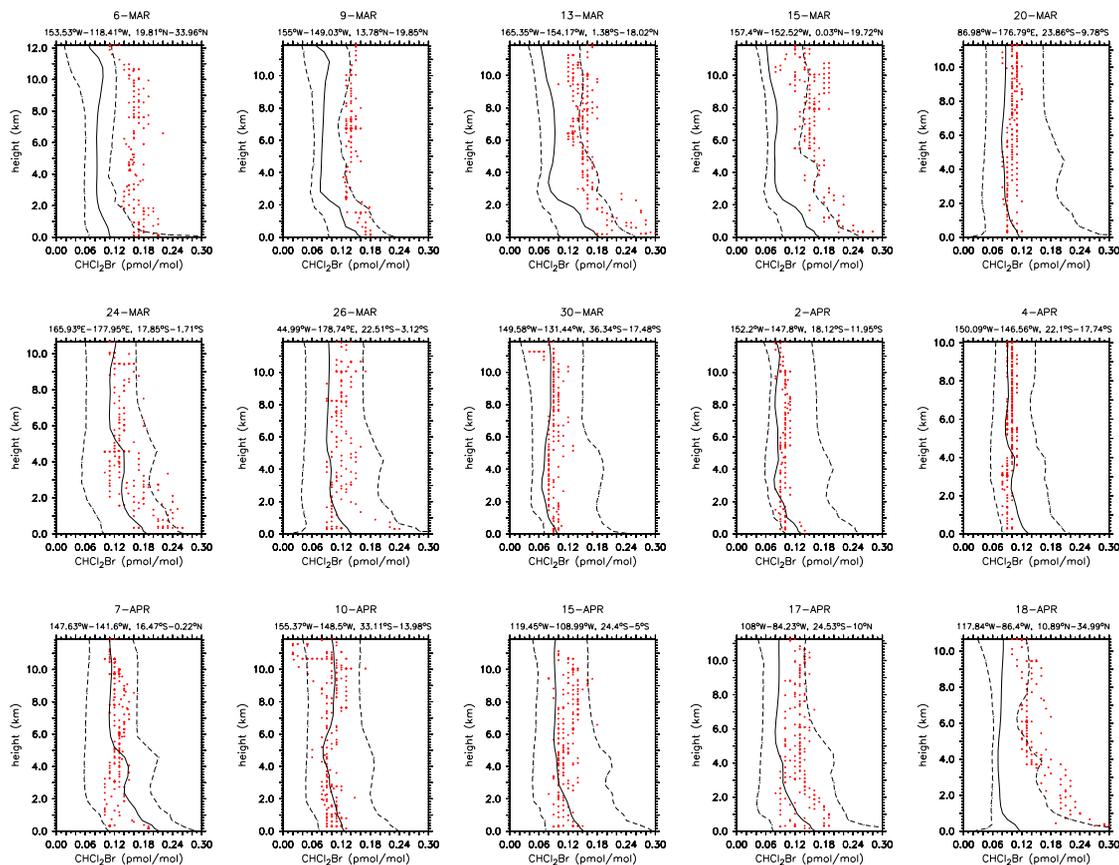
Fig. 15. As Fig. 4 but for CHCl$_2$Br and PEM-Tropics B.

ACPD

8, 9477–9530, 2008

Part 2: Sources of reactive bromine – Bromocarbons

A. Kerkweg et al.

Title Page

Abstract | Introduction

Conclusions | References

Tables | Figures

|◄ | ►|

◄ | ►

Back | Close

Full Screen / Esc

Printer-friendly Version

Interactive Discussion

Fig. 16. As Fig. 4 but for CH$_2$ClBr and PEM-Tropics B.

Title Page

Abstract | Introduction

Conclusions | References

Tables | Figures

|◄ | ►|

◄ | ►

Back | Close

Full Screen / Esc

Printer-friendly Version

Interactive Discussion
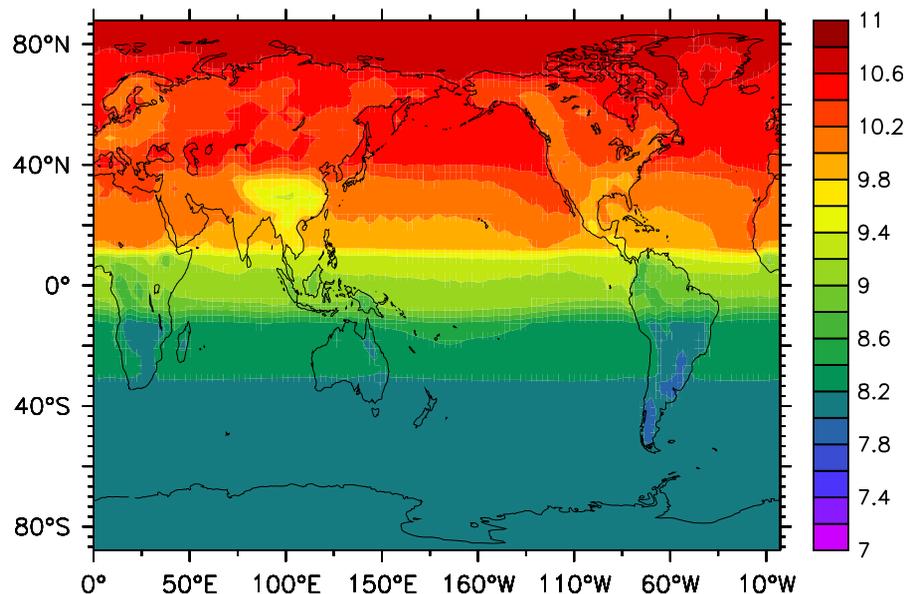
Fig. 17. (a) Annual average of CH_3Br (pmol/mol) in the lowest model layer.
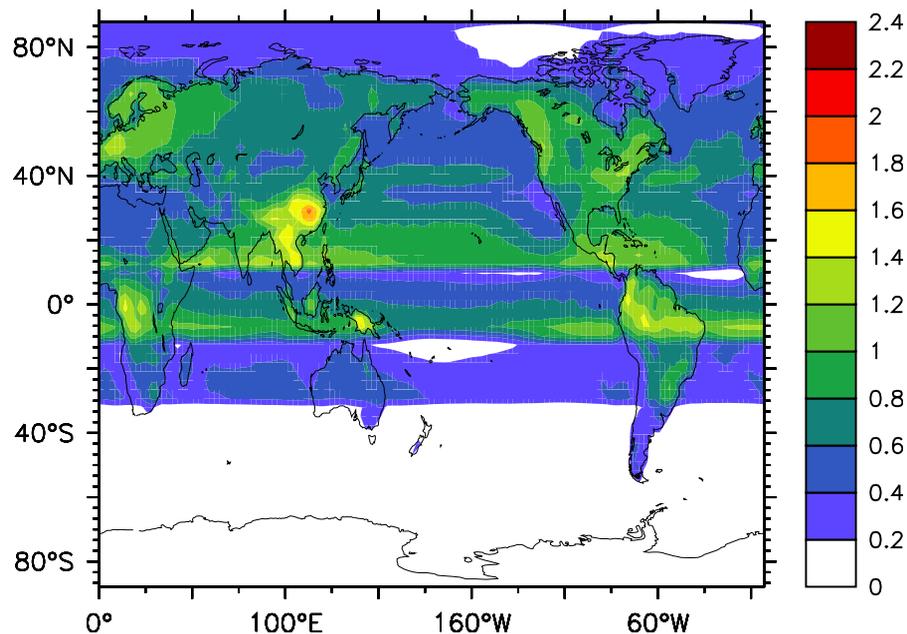
Fig. 18. Annual averages of the CH$_3$Br pseudo-emission flux (10^{11}molecules/(m^{2}s)) resulting from the tracer nudging in the lowest model layer.
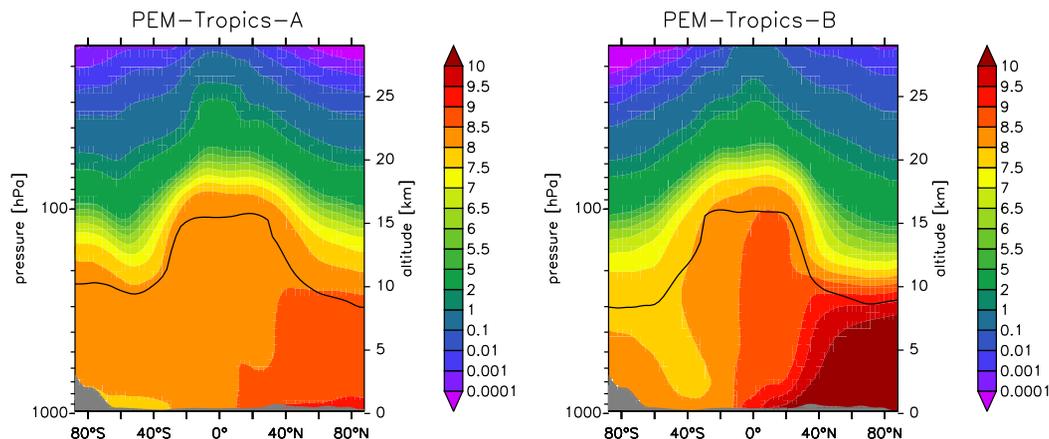
Fig. 19. Zonal averages of simulated CH_3Br mixing ratios (pmol/mol). The periods coincide with the PEM-Tropics A (5 August–6 October) and PEM-Tropics B (6 March–16April) campaigns, though for the year 2000.

Title Page

Abstract | Introduction

Conclusions | References

Tables | Figures

Back | Close

Full Screen / Esc

Printer-friendly Version

Interactive Discussion
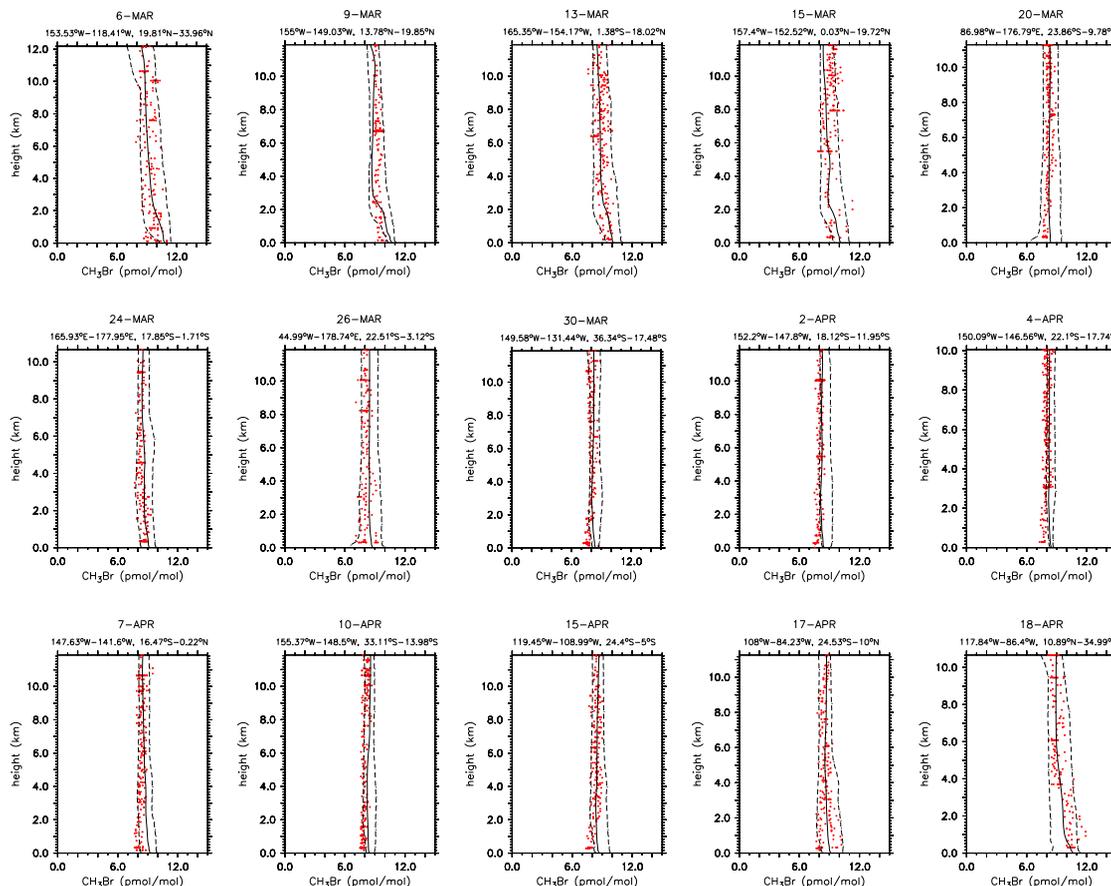
Fig. 20. CH_3Br vertical profiles (pmol/mol) as measured during the PEM-Tropics-B campaign (red dots). The black lines show the simulated vertical profiles averaged over the flight period and area. The dashed lines indicate the simulated minimum and maximum mixing ratios.
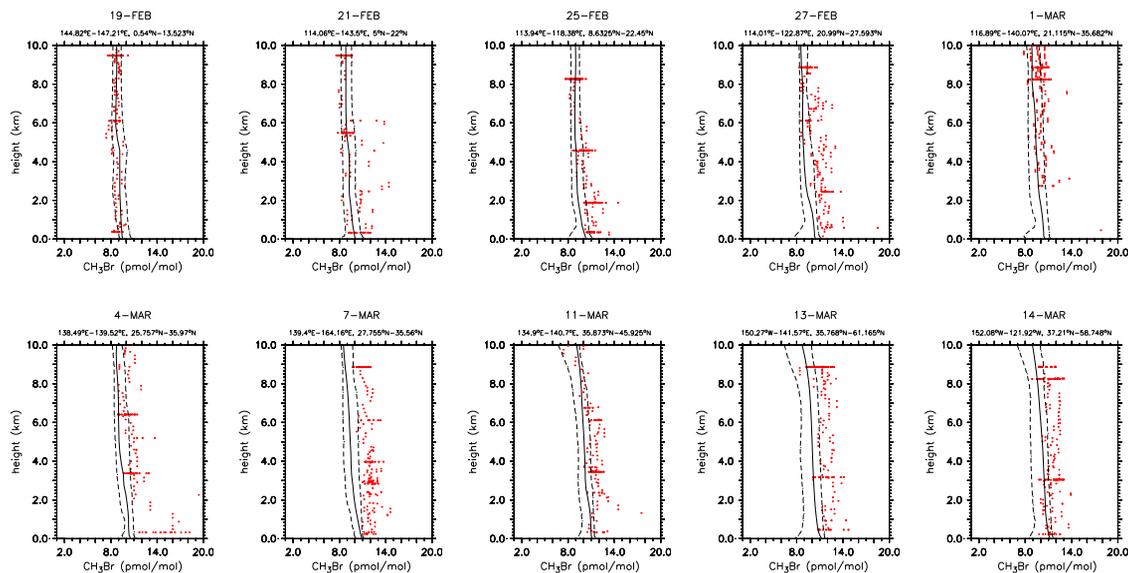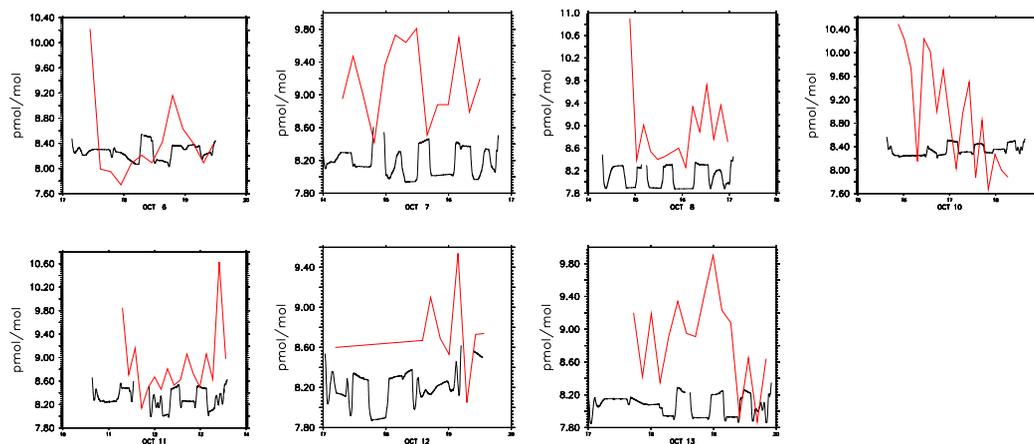
Fig. 21. As Fig. 4 for CH$_3$Br but from PEM-West B.
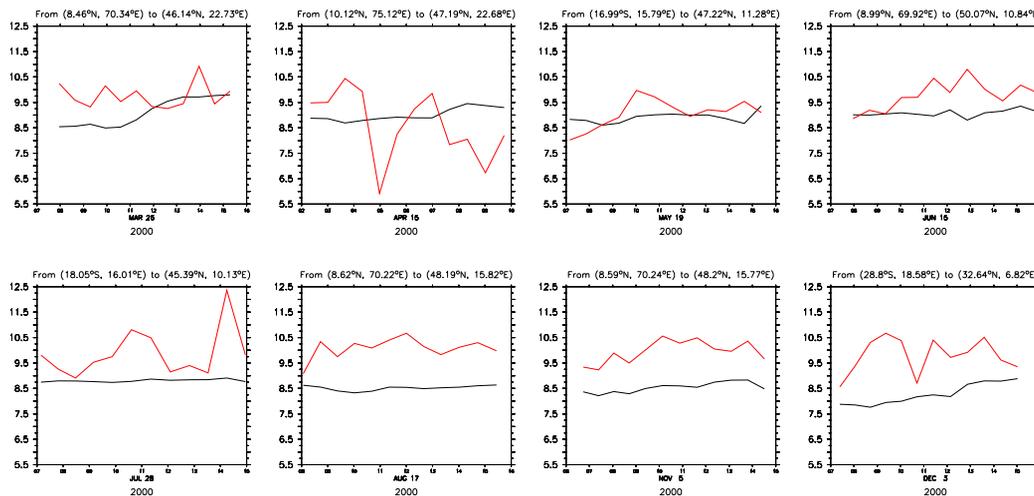
Fig. 22. Point to point comparison of CH_3Br mixing ratios from CARIBIC aircraft data (red line) and model results (black) as a function of time of day from March–December 2000.

Title Page

Abstract | Introduction

Conclusions | References

Tables | Figures

|◄ | ►|

◄ | ►

Back | Close

Full Screen / Esc

Printer-friendly Version

Interactive Discussion

Fig. 23. Point to point comparison of CH_3Br mixing ratios from GABRIEL aircraft data (red line) and model results (black) as a function of time of day in October 2000.
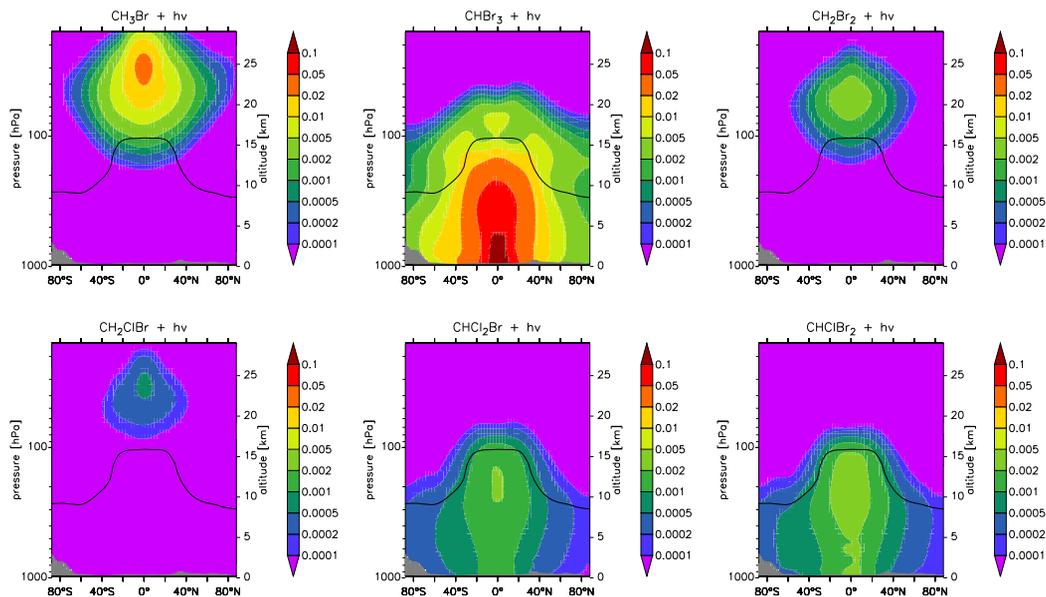
Fig. 24. Simulated production of Br radicals in g(Br)/s by photolysis of bromocarbons
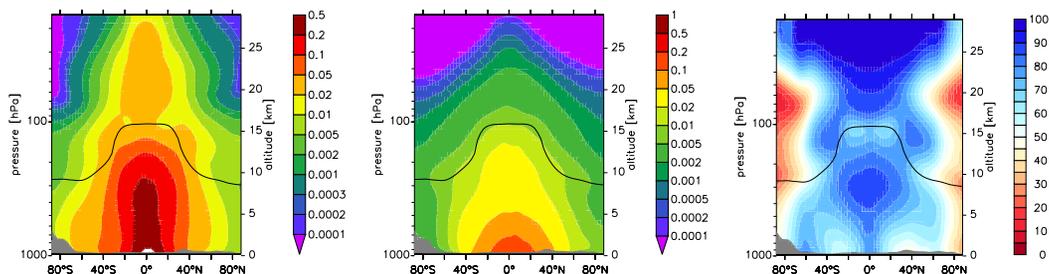
Fig. 25. Simulated zonally averaged Br radical production (in pmol/mol/day) by photolysis (left) and reaction with OH (middle) of bromocarbons, respectively. Here, photolysis of all six discussed bromocarbons and halons are taken into account. Right: Fraction (in%) of Br generated by photolysis to total Br production (photolysis+reaction with OH) from bromocarbons.